Parameterized flows: examples of convergence between data and computational science

Angelo Iollo

work with M. Bergmann, F. Bernard, C. Farhat, S. Grimberg, S. Riffaud, A. Scardigli, H. Telib, T. Taddei

Institut de Mathématiques de Bordeaux, Université de Bordeaux
Memphis Team, Inria Bordeaux - Sud Ouest

Réduction de modèles et traitement géométrique des données
Paris - November 8-9, 2021

université de BORDEAUX

Inria

cnrs

Old & New

Hybrid FO-RO numerical model: DD and ML

PDE model to be solved for u in Ω: $D(u(x)) = 0$, $x \in \Omega$

Hybrid FO-RO numerical model: DD and ML

PDE model to be solved for u in Ω: $D(u(x)) = 0$, $x \in \Omega$

- Partition Ω so that $\Omega = \bigcup_{i=1}^{M} \Omega_i$ and $\Omega_i \bigcap \Omega_j \neq \emptyset$ for some $i, j \in \{1, \ldots, M\}$, $i \neq j$

Hybrid FO-RO numerical model: DD and ML

PDE model to be solved for u in Ω: $D(u(x)) = 0$, $x \in \Omega$

- Partition Ω so that $\Omega = \bigcup_{i=1}^{M} \Omega_i$ and $\Omega_i \bigcap \Omega_j \neq \emptyset$ for some $i, j \in \{1, \ldots, M\}$, $i \neq j$
- Define in Ω_i an approximation space $V_i = \text{Span}\left\{\phi_1^i, \ldots, \phi_k^i, \ldots\right\}$, $\dim(V_i) = N_i$

Hybrid FO-RO numerical model: DD and ML

PDE model to be solved for u in Ω: $D(u(x)) = 0,\ x \in \Omega$

- Partition Ω so that $\Omega = \bigcup_{i=1}^{M} \Omega_i$ and $\Omega_i \bigcap \Omega_j \neq \emptyset$ for some $i, j \in \{1, \ldots, M\},\ i \neq j$
- Define in Ω_i an approximation space $V_i = \text{Span}\left\{\phi_1^i, \ldots, \phi_k^i, \ldots\right\}$, $\dim(V_i) = N_i$
- Let $\tilde{u}_i(x) = \sum_{k=1}^{N_i} a_k^i\, \phi_k^i(x)$ and $A = (a_1^1, \ldots, a_i^j, \ldots)$; $\dim(A) = \sum_{i=1}^{M} N_i$

Hybrid FO-RO numerical model: DD and ML

PDE model to be solved for u in Ω: $D(u(x)) = 0,\ x \in \Omega$

- Partition Ω so that $\Omega = \bigcup_{i=1}^{M} \Omega_i$ and $\Omega_i \bigcap \Omega_j \neq \emptyset$ for some $i, j \in \{1, \ldots, M\},\ i \neq j$
- Define in Ω_i an approximation space $V_i = \text{Span}\left\{\phi_1^i, \ldots, \phi_k^i, \ldots\right\}$, $\dim(V_i) = N_i$
- Let $\tilde{u}_i(x) = \sum_{k=1}^{N_i} a_k^i\, \phi_k^i(x)$ and $A = (a_1^1, \ldots, a_i^j, \ldots)$; $\dim(A) = \sum_{i=1}^{M} N_i$
- Define the residuals in Ω: $\mathcal{R}(A, x) = \mathcal{R}(D(\tilde{u}_1(x)), \ldots, D(\tilde{u}_M(x)))$

Hybrid FO-RO numerical model: DD and ML

PDE model to be solved for u in Ω: $D(u(x)) = 0,\ x \in \Omega$

- Partition Ω so that $\Omega = \bigcup_{i=1}^{M} \Omega_i$ and $\Omega_i \bigcap \Omega_j \neq \emptyset$ for some $i, j \in \{1, \ldots, M\},\ i \neq j$
- Define in Ω_i an approximation space $V_i = \text{Span}\left\{\phi_1^i, \ldots, \phi_k^i, \ldots\right\}$, $\dim(V_i) = N_i$
- Let $\tilde{u}_i(x) = \sum_{k=1}^{N_i} a_k^i\, \phi_k^i(x)$ and $A = (a_1^1, \ldots, a_i^j, \ldots)$; $\dim(A) = \sum_{i=1}^{M} N_i$
- Define the residuals in Ω: $\mathcal{R}(A, x) = \mathcal{R}(D(\tilde{u}_1(x)), \ldots, D(\tilde{u}_M(x)))$
- Solve $f\left(\mathcal{R}\right)(A) = 0$

Hybrid FO-RO numerical model: DD and ML

PDE model to be solved for u in Ω: $D(u(x)) = 0,\ x \in \Omega$

- Partition Ω so that $\Omega = \bigcup_{i=1}^{M} \Omega_i$ and $\Omega_i \bigcap \Omega_j \neq \emptyset$ for some $i, j \in \{1, \ldots, M\},\ i \neq j$
- Define in Ω_i an approximation space $V_i = \text{Span}\left\{\phi_1^i, \ldots, \phi_k^i, \ldots\right\}$, $\dim(V_i) = N_i$
- Let $\tilde{u}_i(x) = \sum_{k=1}^{N_i} a_k^i\, \phi_k^i(x)$ and $A = (a_1^1, \ldots, a_i^j, \ldots)$; $\dim(A) = \sum_{i=1}^{M} N_i$
- Define the residuals in Ω: $\mathcal{R}(A, x) = \mathcal{R}(D(\tilde{u}_1(x)), \ldots, D(\tilde{u}_M(x)))$
- Solve $f\left(\mathcal{R}\right)(A) = 0$

Learning on previously collected solutions

Hybrid FO-RO numerical model: DD and ML

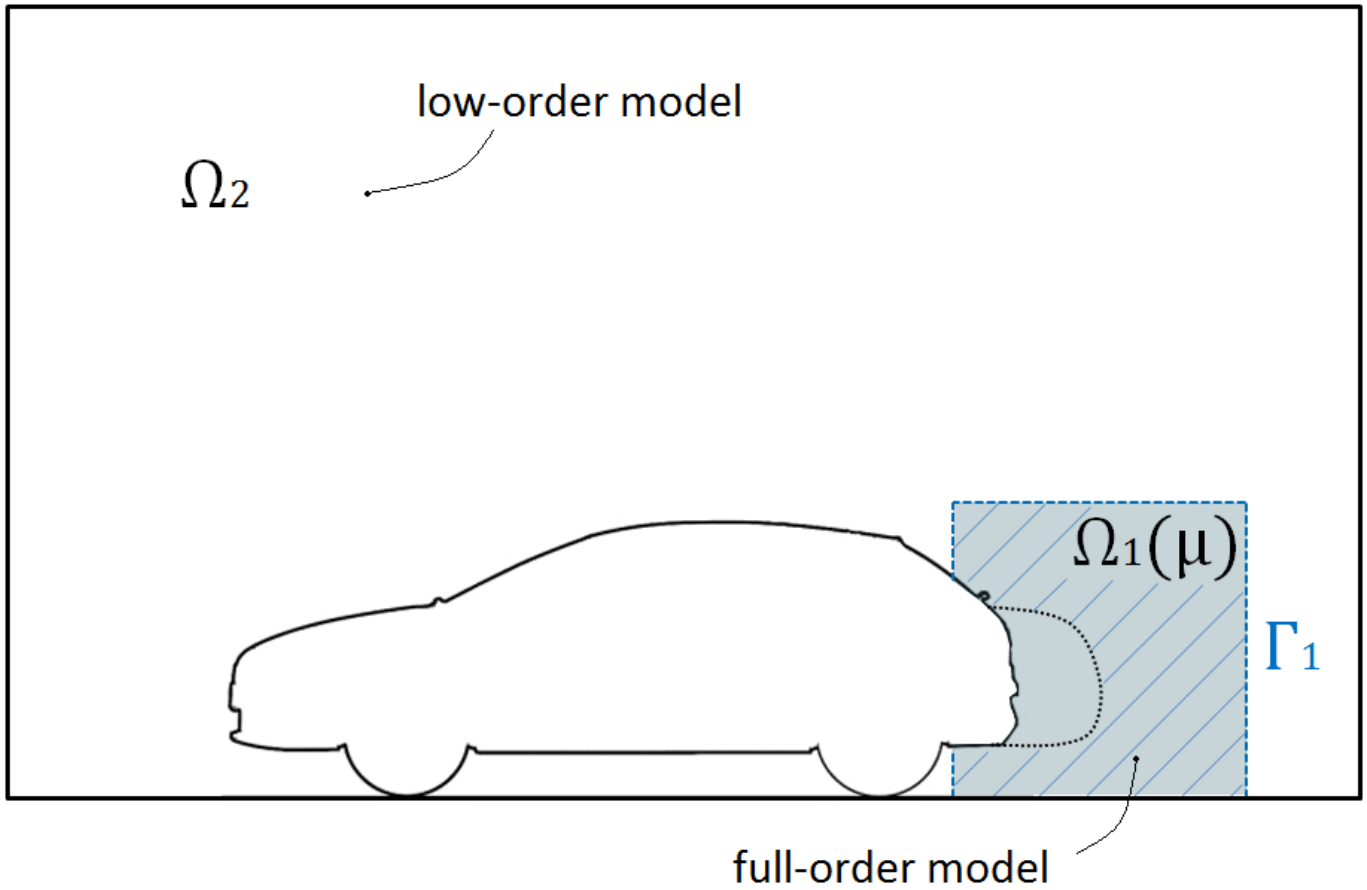
PDE model to be solved for u in Ω: $D(u(x)) = 0,\ x \in \Omega$

- Partition Ω so that $\Omega = \bigcup_{i=1}^{M} \Omega_i$ and $\Omega_i \bigcap \Omega_j \neq \emptyset$ for some $i, j \in \{1, \ldots, M\},\ i \neq j$
- Define in Ω_i an approximation space $V_i = \text{Span}\left\{\phi_1^i, \ldots, \phi_k^i, \ldots\right\}$, $\dim(V_i) = N_i$
- Let $\tilde{u}_i(x) = \sum_{k=1}^{N_i} a_k^i\, \phi_k^i(x)$ and $A = (a_1^1, \ldots, a_i^j, \ldots)$; $\dim(A) = \sum_{i=1}^{M} N_i$
- Define the residuals in Ω: $\mathcal{R}(A, x) = \mathcal{R}(D(\tilde{u}_1(x)), \ldots, D(\tilde{u}_M(x)))$
- Solve $f\left(\mathcal{R}\right)(A) = 0$

Learning on previously collected solutions

M. Buffoni, H. Telib, A.I. C&F 2006
M. Bergmann, A. Ferrero, A.I., E. Lombardi, H. Telib JCP 2018
S. Riffaud, M. Bergmann, C. Farhat, S. Grimberg, A.I. JCP 2021

Domain decomposition: RANS equations

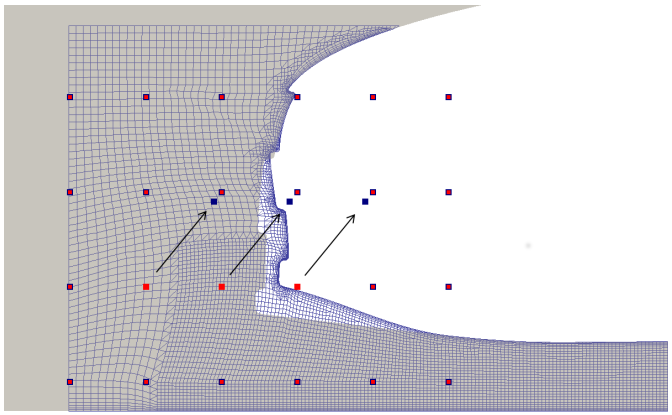


$\Omega_1(\mu)$ FOM model
Ω_2 Reduced model used to define non-local boundary conditions on Γ_1
$N_1 >> N_2$ and for example $\phi_k^1 \in P_1(W_k)$, $\phi_k^2 \in \{\text{POD subspace}\}$

2D DrivAer car model

Domain L×H=50m×12m, $U_\infty = 16\text{m/s}$, $l_{ref} = 4.61\text{m}$
RANS simulations: Spalart-Allmaras turbulence model at $Re = 4.87\,10^6$
FFD parametrization of car front bumper $\boldsymbol{\mu} = (\mu_0, \mu_1)$



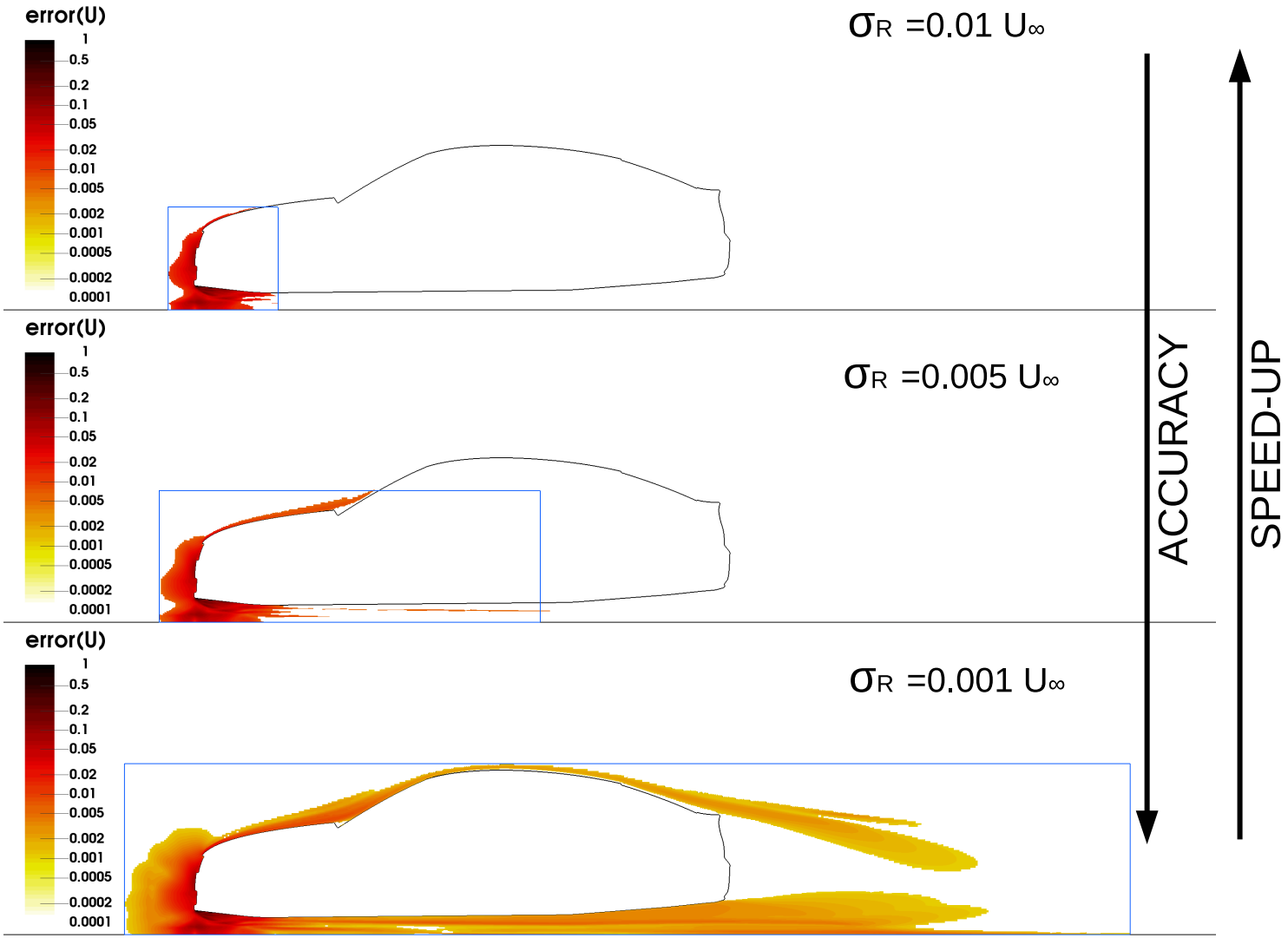


Sampling
Data driven selection of Ω_1 and Ω_2
Convergence

Decomposition threshold: error indicator

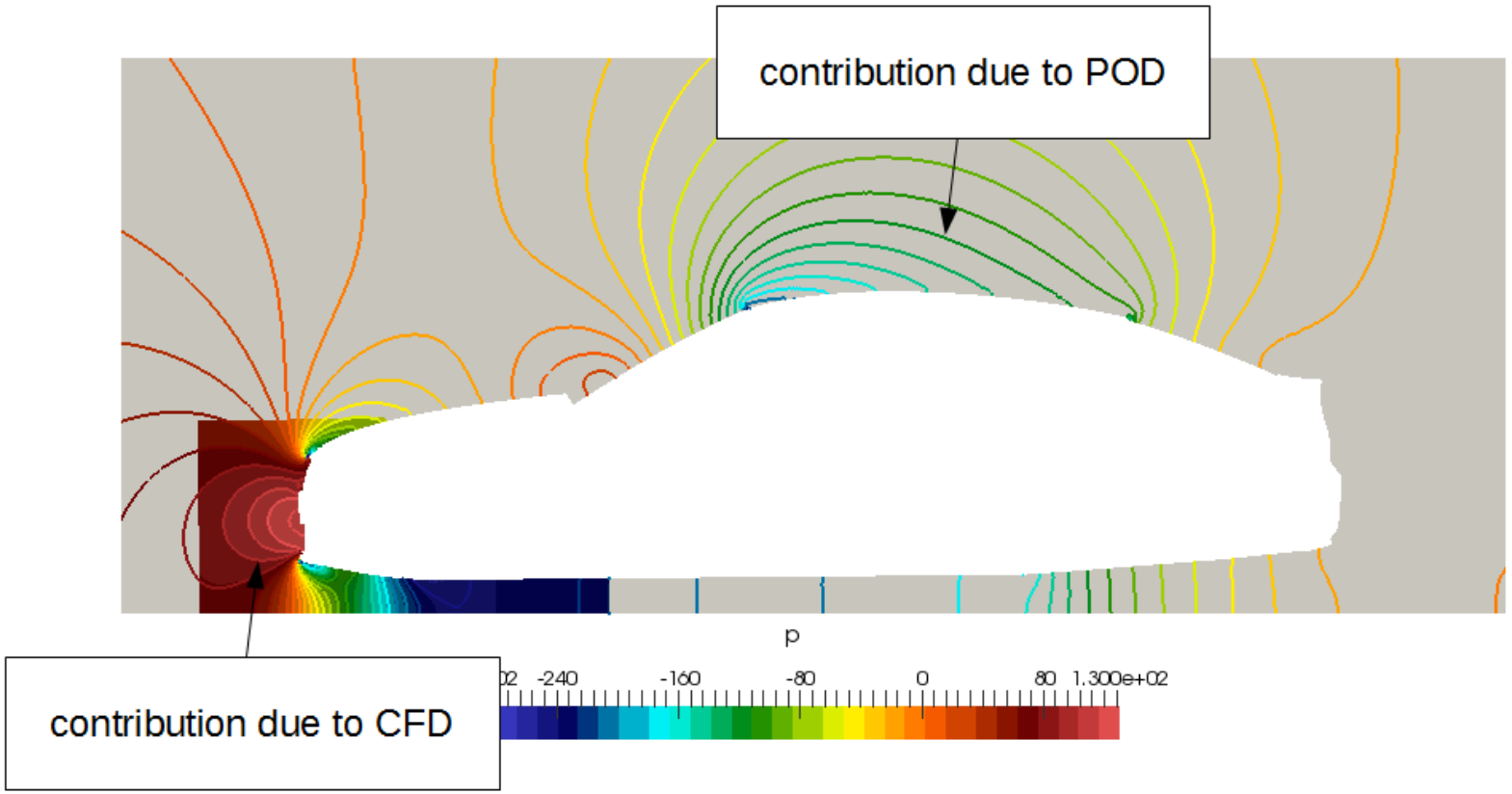
Let $\mathcal{S}$ the learning set and $\mathcal{P}_s$ the projection operator in $\mathcal{S}\backslash s$

$$e(x) = \max_{s \in \mathcal{S}} |u_s(x) - \mathcal{P}_s(u_s(x))|$$



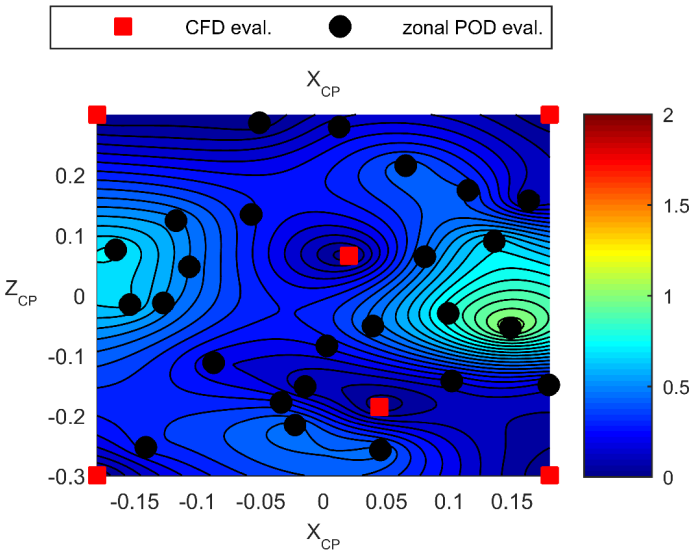
Drag coefficient

The goal function, i.e. the overall drag coefficient, is given by the sum of 2 contributions



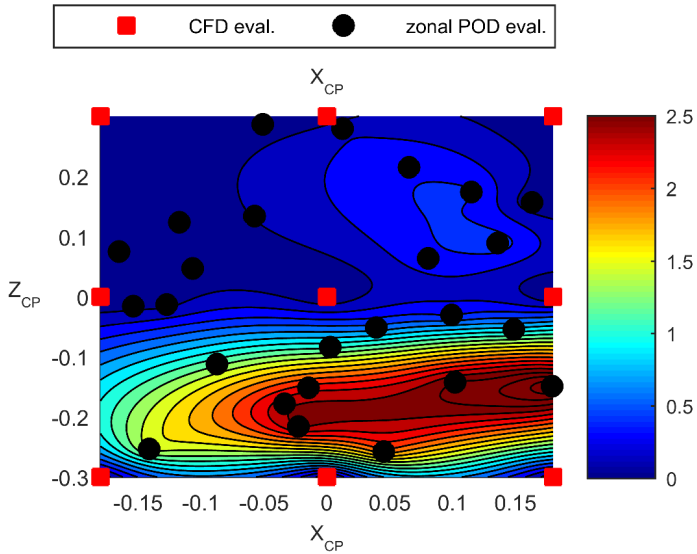
Accuracy

Greedy sampling vs uniform sampling



N=5
Ns=6

ε=0.4271%

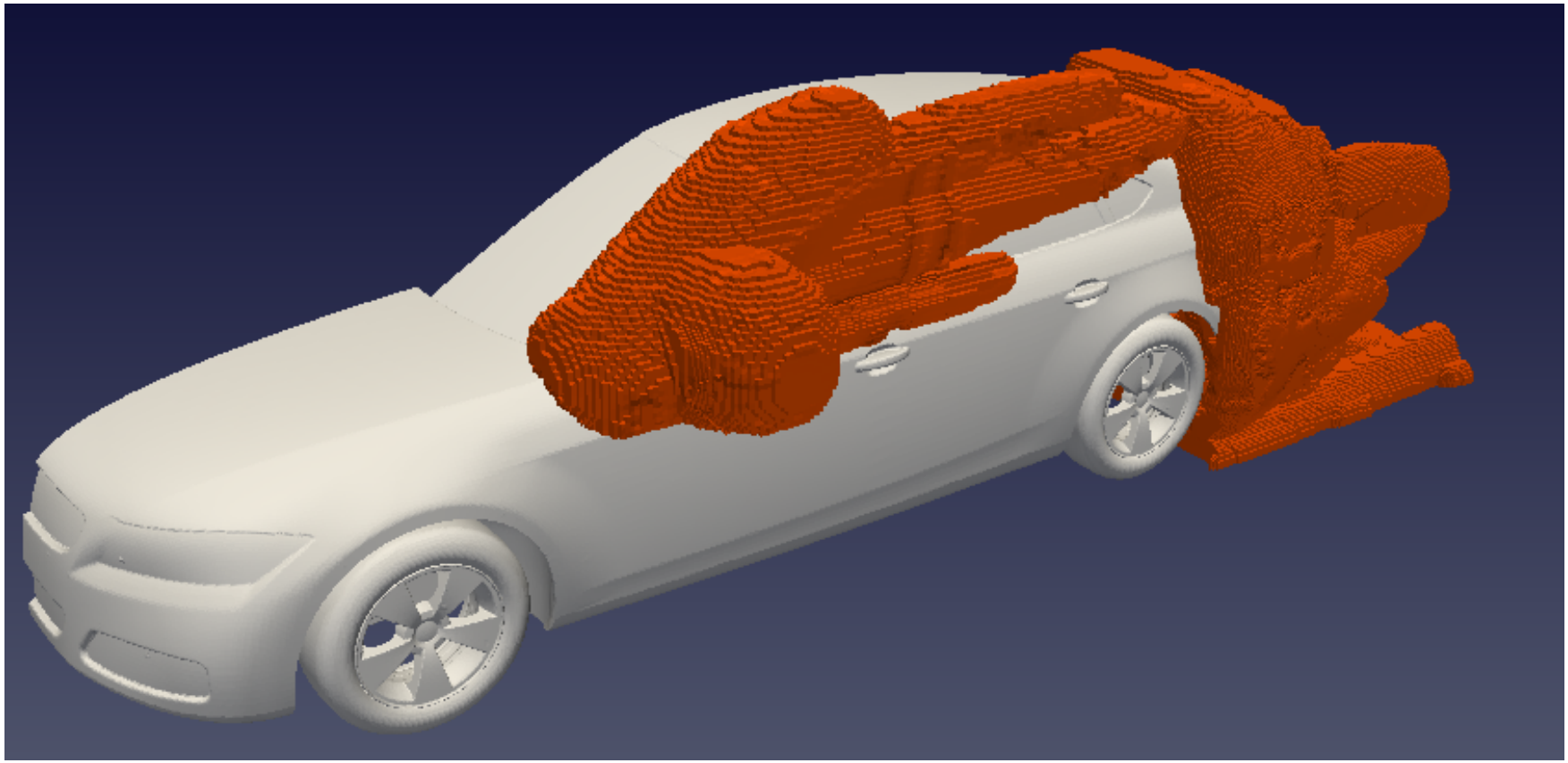


N=8
Ns=9

ε=0.9341%

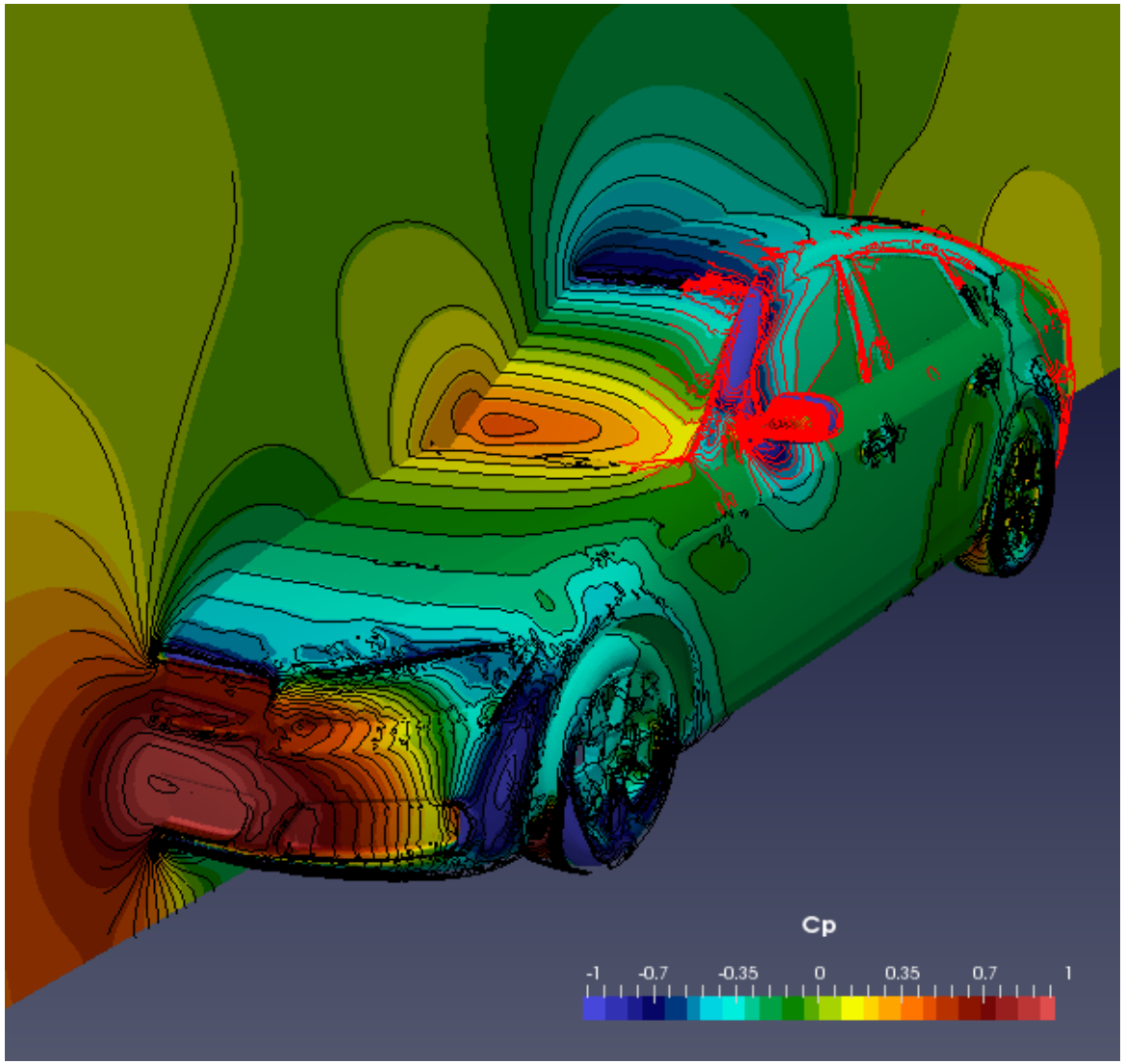
the ensemble-averaged error ϵ is halved using 6 snapshots instead of 9

Rear mirror design



domain decomposition

Rear mirror design



POD (black isolines) + CFD (red isolines) and full CFD solution (colormap)

Old and New: Domain Decomposition and Machine Learning

PDE model to be solved for u in Ω: $D(u(x)) = 0,\ x \in \Omega$

- Partition Ω so that $\Omega = \bigcup_{i=1}^{M} \Omega_i$ and $\Omega_i \bigcap \Omega_j \neq \emptyset$ for some $i, j \in \{1, \ldots, M\},\ i \neq j$
- Define in Ω_i an approximation space $V_i = \text{Span}\left\{\phi_1^i, \ldots, \phi_k^i, \ldots\right\}$, $\dim(V_i) = N_i$
- Let $\tilde{u}_i(x) = \sum_{k=1}^{N_i} a_k^i \, \phi_k^i(x)$ and $A = (a_1^1, \ldots, a_i^j, \ldots)$; $\dim(A) = \sum_{i=1}^{M} N_i$
- Define the residuals in Ω: $\mathcal{R}(A, x) = \mathcal{R}(D(\tilde{u}_1(x)), \ldots, D(\tilde{u}_M(x)))$
- Solve $f\left(\mathcal{R}\right)(A) = 0$

Learning on previously collected solutions

Learning where to compute the residuals: Euler equations

We consider the modeling of inviscid compressible flow governed by the **2D Euler equations**:

$$\frac{\partial \mathsf{q}}{\partial t} + \nabla \cdot \mathsf{F}(\mathsf{q}) = 0,$$

where q denotes the conservative state variable and $\mathsf{F} = (\mathsf{f}, \mathsf{g})$ denotes the flux, with

$$\mathsf{q} = \begin{pmatrix} \rho \\ \rho u \\ \rho v \\ E \end{pmatrix}, \quad \mathsf{f} = \begin{pmatrix} \rho u \\ \rho u^2 + p \\ \rho uv \\ u(E+p) \end{pmatrix}, \quad \mathsf{g} = \begin{pmatrix} \rho v \\ \rho uv \\ \rho v^2 + p \\ v(E+p) \end{pmatrix},$$

where ρ is the density, $(u, v)^T$ is the velocity, E is the total energy and p is the pressure.

Reduced-order model

- Each component of the solution is approximated in space by basis functions Φ_n^i

$$\widetilde{q}_i(x,t;\mu) = q_o^i(x) + \sum_{n=1}^{M_i} a_n^i(t;\mu)\Phi_n^i(x)$$

Reduced-order model

- Each component of the solution is approximated in space by basis functions Φ_n^i

$$\widetilde{q}_i(x,t;\mu) = q_o^i(x) + \sum_{n=1}^{M_i} a_n^i(t;\mu)\Phi_n^i(x)$$

- the reduced coordinates a_n^i are determined in the prediction stage by DG

$$\frac{\mathrm{d}a_n^i}{\mathrm{d}t} = \sum_{K\in\Omega}\left(\int_K \mathsf{F}_i(\widetilde{\mathsf{q}})\cdot\nabla\Phi_n^i - \int_{\partial K}\widehat{F}_i(\widetilde{\mathsf{q}}^-,\widetilde{\mathsf{q}}^+,\mathsf{n})\Phi_n^i\,\mathrm{d}\boldsymbol{\sigma}\right)$$

Reduced-order model

- Each component of the solution is approximated in space by basis functions Φ_n^i

$$\widetilde{q}_i(x,t;\mu) = q_o^i(x) + \sum_{n=1}^{M_i} a_n^i(t;\mu)\Phi_n^i(x)$$

- the reduced coordinates a_n^i are determined in the prediction stage by DG

$$\frac{\mathrm{d}a_n^i}{\mathrm{d}t} = \sum_{K\in\Omega}\left(\int_K \mathsf{F}_i(\widetilde{\mathsf{q}})\cdot\nabla\Phi_n^i - \int_{\partial K}\widehat{F}_i(\widetilde{\mathsf{q}}^-,\widetilde{\mathsf{q}}^+,\mathsf{n})\Phi_n^i\,\mathrm{d}\boldsymbol{\sigma}\right)$$

- To evaluate the volume integral in principle we should compute the integrand

$$H_{i,n}^v[\widetilde{\mathsf{q}}] = \mathsf{F}_i(\widetilde{\mathsf{q}})\cdot\nabla\Phi_n^i$$

at each point $\mathsf{x}\in\bigcup_{K\in\Omega} K$.

Reduced-order model

- Each component of the solution is approximated in space by basis functions Φ_n^i

$$\widetilde{q}_i(x,t;\mu) = q_o^i(x) + \sum_{n=1}^{M_i} a_n^i(t;\mu)\Phi_n^i(x)$$

- the reduced coordinates a_n^i are determined in the prediction stage by DG

$$\frac{\mathrm{d}a_n^i}{\mathrm{d}t} = \sum_{K\in\Omega}\left(\int_K \mathsf{F}_i(\widetilde{\mathsf{q}})\cdot\nabla\Phi_n^i - \int_{\partial K}\widehat{F}_i(\widetilde{\mathsf{q}}^-,\widetilde{\mathsf{q}}^+,\mathsf{n})\Phi_n^i\,\mathrm{d}\boldsymbol{\sigma}\right)$$

- To evaluate the volume integral in principle we should compute the integrand

$$H_{i,n}^v[\widetilde{\mathsf{q}}] = \mathsf{F}_i(\widetilde{\mathsf{q}})\cdot\nabla\Phi_n^i$$

  at each point $\mathsf{x}\in\bigcup_{K\in\Omega} K$.

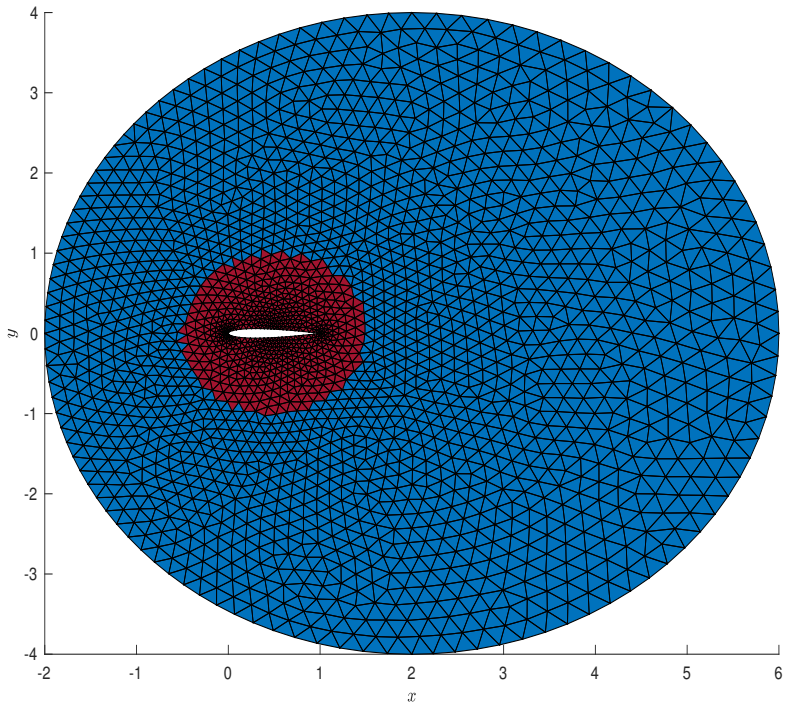
- Instead, the volume integrals are approximated as

$$\int_{\bigcup_{K\in\Omega} K} H_{i,n}^v[\widetilde{\mathsf{q}}](\mathsf{x})\,\mathrm{d}\mathsf{x} \approx \sum_{l=1}^{L_v}\widetilde{\omega}_l^v H_{i,n}^v[\widetilde{\mathsf{q}}](\widetilde{\mathsf{x}}_l),$$

  where $\widetilde{\omega}_l^v > 0$ is the weight associated to the point $\widetilde{\mathsf{x}}_l$ and $L_v \ll N_{\mathsf{x}}$

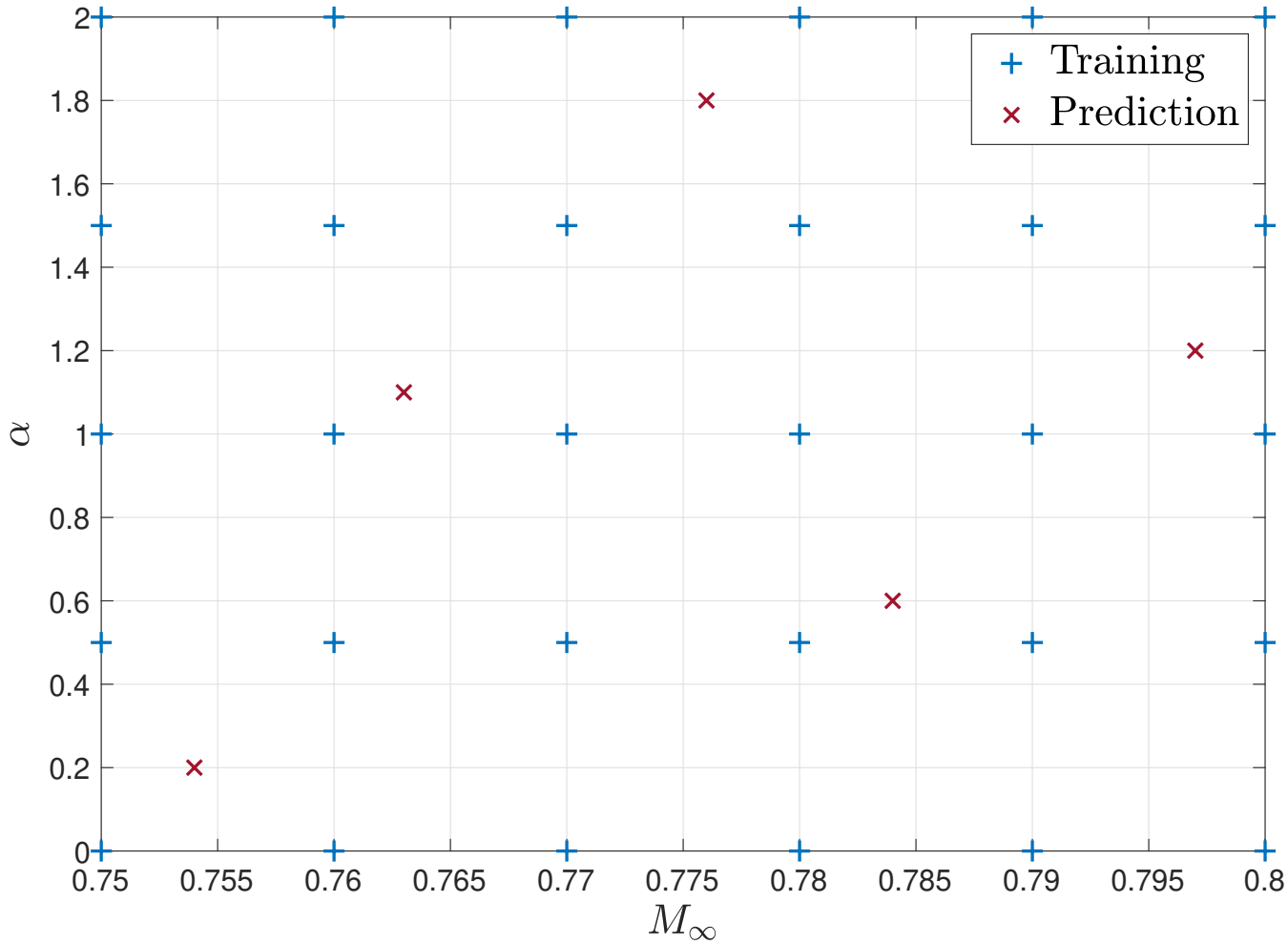
Prediction of a transonic flow

- The input parameters $\mu = (M_\infty, \alpha)$ correspond to different free-stream Mach numbers M_∞ and angles of attack α.
- The 2D Euler equations are discretized using a 2^{nd}-order DG method equipped with the HLL flux and the BJ limiter in space and the 2^{nd}-order TVD Runge-Kutta scheme in time.



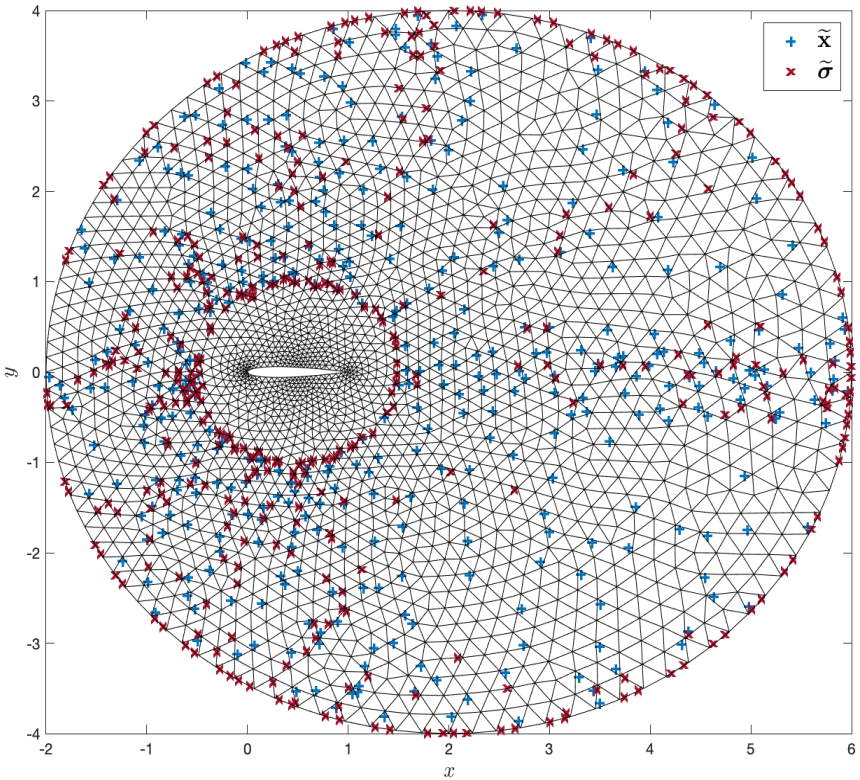
Decomposition of the domain in two subdomains.

Prediction of a transonic flow: learning set



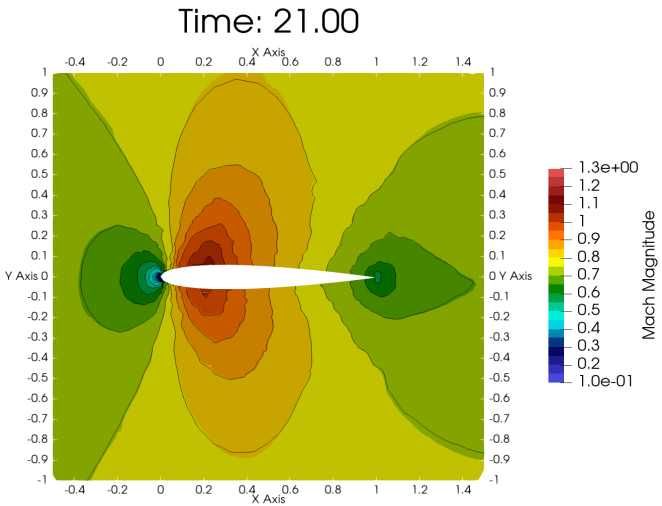
Prediction of a transonic flow

- The ECSW procedure identifies 403 (resp. 629) points $\widetilde{x}_l$ (resp. $\widetilde{\sigma}_l$) among the 9255 (resp. 9314) quadrature points to evaluate the volume (resp. surface) integrals.

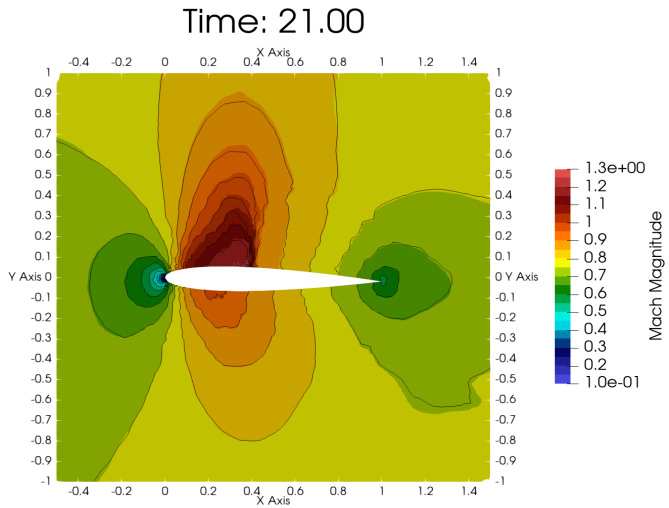


Quadrature points delivered by the ECSW method.

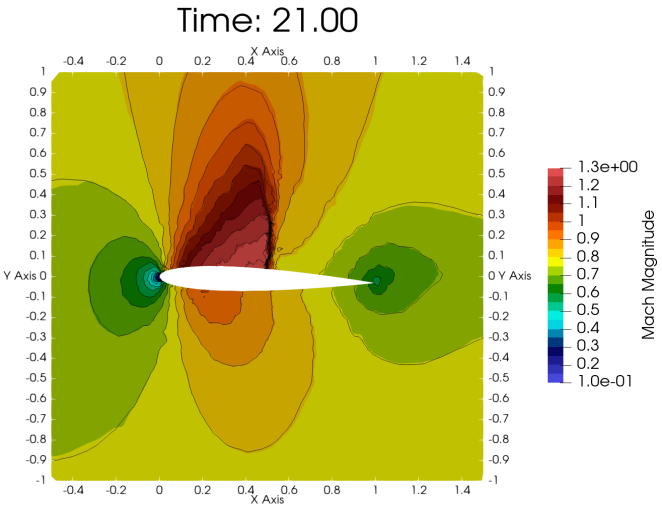
Prediction of a transonic flow



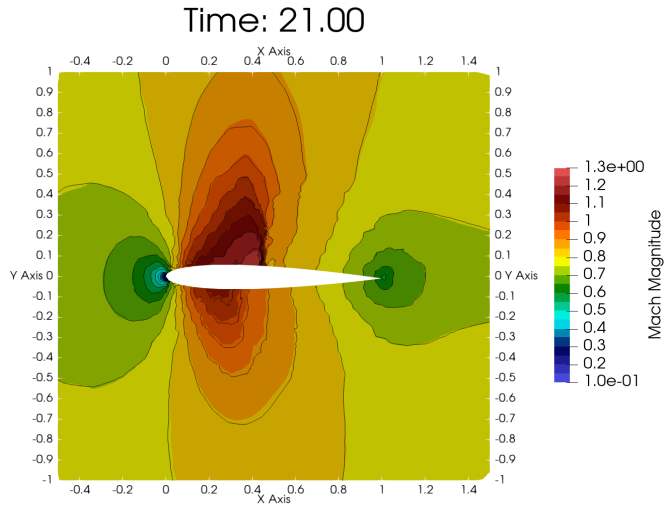
(a) $\mu = (0.754, 0.2)$



(b) $\mu = (0.763, 1.1)$

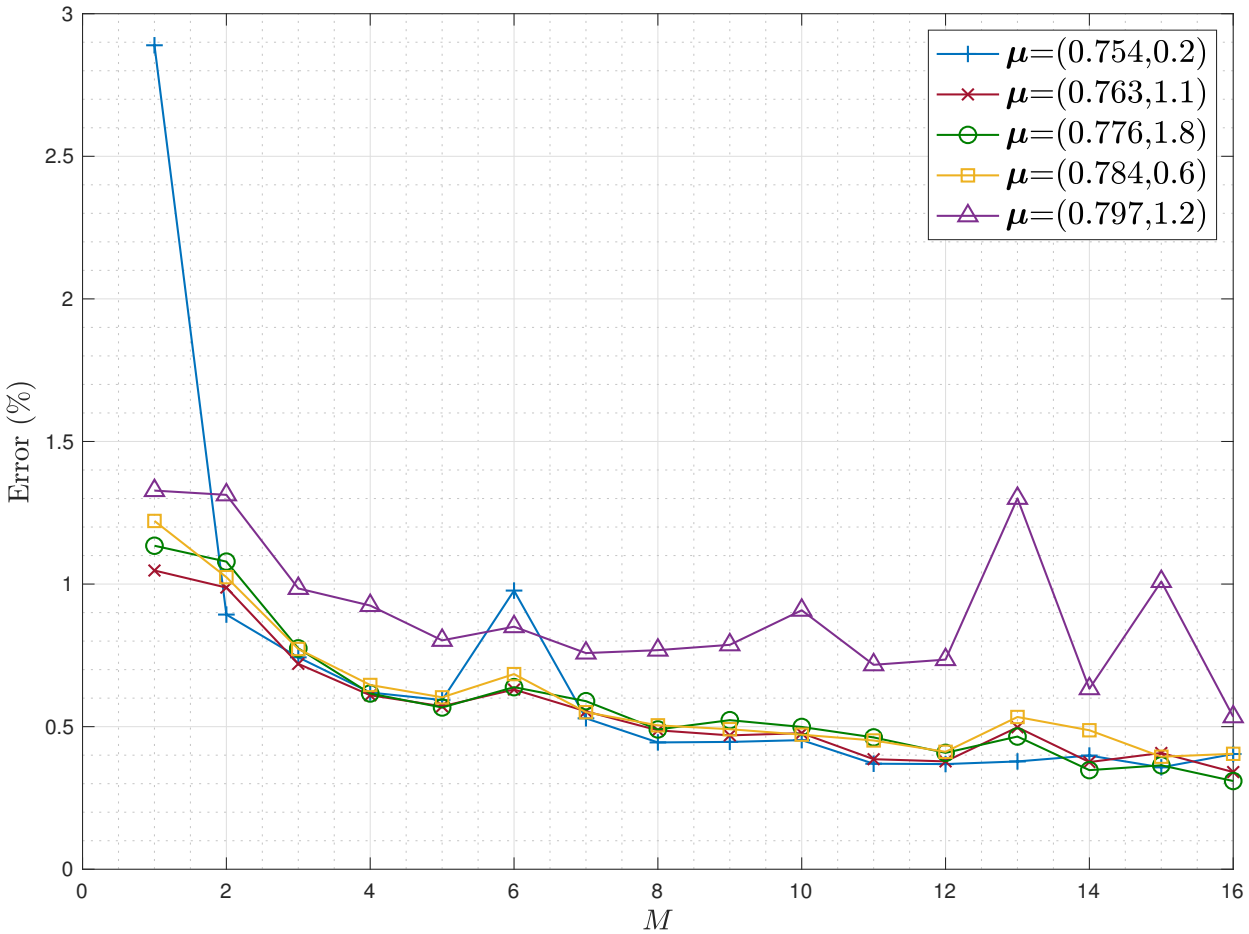


(c) $\mu = (0.776, 1.8)$



(d) $\mu = (0.784, 0.6)$

Prediction of a transonic flow



Error of the prediction tests for the transonic NACA airfoil problem.

Data augmentation

Intermission: Monge problem

- Given two unit densities $\rho_0(\xi)$ and $\rho_1(x)$ in $\mathbb{R}^d$, the Monge problem (Théorie des Déblais & des Remblais, 1781 or the Monge barrow) of optimal transportation defines a distance:

$$d^2(\rho_1, \rho_0) = \inf_X \int_{\mathbb{R}^d} \rho_0(\xi) \left(X(\xi) - \xi\right)^2 d\xi$$

subject to mass conservation:

$$\rho_0(\xi) = \rho_1(X(\xi)) \det\left(\nabla X(\xi)\right)$$

Intermission: Monge problem

- Given two unit densities $\rho_0(\xi)$ and $\rho_1(x)$ in $\mathbb{R}^d$, the Monge problem (Théorie des Déblais & des Remblais, 1781 or the Monge barrow) of optimal transportation defines a distance:

$$d^2(\rho_1, \rho_0) = \inf_X \int_{\mathbb{R}^d} \rho_0(\xi) \left(X(\xi) - \xi\right)^2 d\xi$$

  subject to mass conservation:

$$\rho_0(\xi) = \rho_1(X(\xi)) \det\left(\nabla X(\xi)\right)$$

- Let $X^*(\xi)$ the optimal map, the geodesic map $\gamma(t) = (1-t)\,\xi + t\,X^*(\xi)$, $0 \leq t \leq 1$ defines a set of interpolated densities

Intermission: Monge problem

- Given two unit densities $\rho_0(\xi)$ and $\rho_1(x)$ in $\mathbb{R}^d$, the Monge problem (Théorie des Déblais & des Remblais, 1781 or the Monge barrow) of optimal transportation defines a distance:

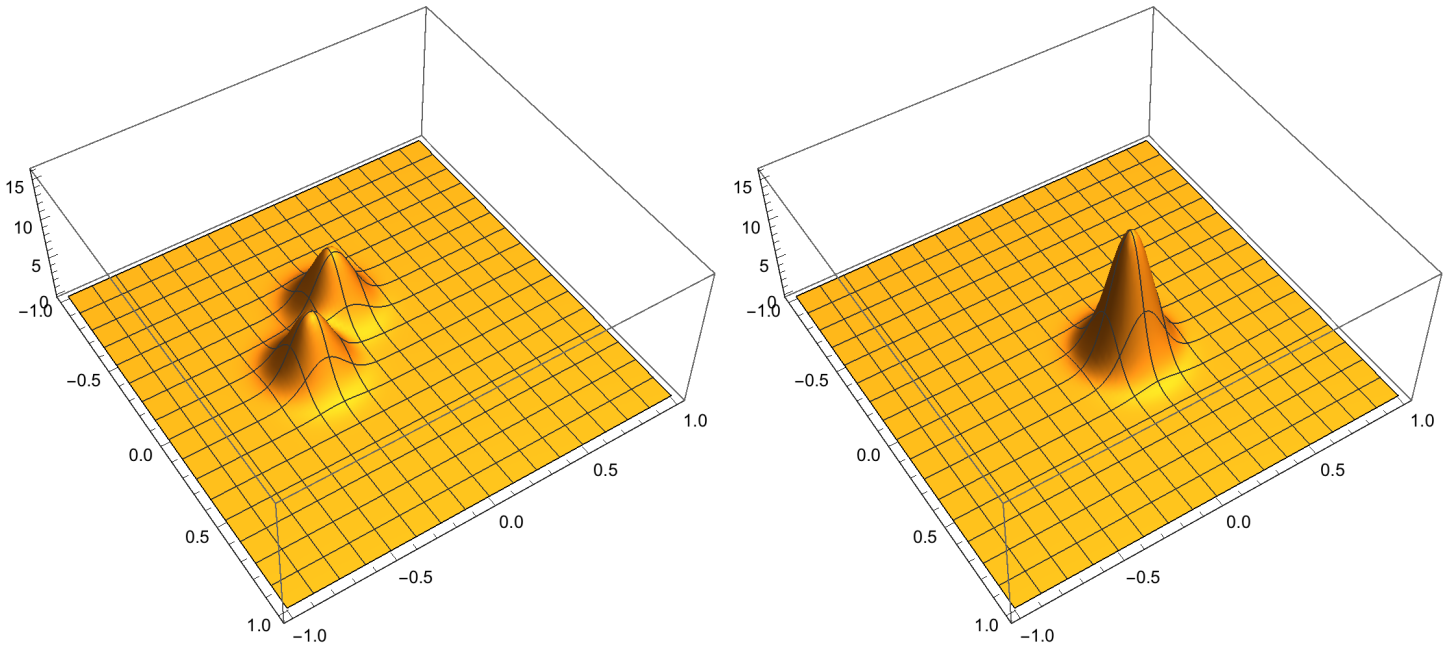
$$d^2(\rho_1, \rho_0) = \inf_X \int_{\mathbb{R}^d} \rho_0(\xi) \, (X(\xi) - \xi)^2 \, d\xi$$

  subject to mass conservation:

$$\rho_0(\xi) = \rho_1(X(\xi)) \det(\nabla X(\xi))$$

- Let $X^*(\xi)$ the optimal map, the geodesic map $\gamma(t) = (1-t)\,\xi + t\,X^*(\xi)$, $0 \leq t \leq 1$ defines a set of interpolated densities
- Existence and unicity of the solution X but difficult to find. Densities can be found with entropy regularization $\Rightarrow$ Kullback-Leibler divegrence

Geodesic interpolation



Geodesic interpolation

A textbook case of data augmentation by OT: BGK kinetic model

Linear transport in microscopic velocity space with non-linear relaxation to equilibrium

$$\frac{\partial f}{\partial t}(x,\xi,t) + \xi \cdot \nabla_x f(x,\xi,t) = \frac{M_f(x,\xi,t) - f(x,\xi,t)}{\tau(x,t)}$$

f is the density distribution function. Maxwell equilibrium distribution function:

$$M_f(x,\xi,t) = \frac{\rho(x,t)}{(2\pi T(x,t))^{\frac{3}{2}}} \exp\left(-\frac{|\xi - U(x,t)|^2}{2T(x,t)}\right)$$

The macroscopic variables are:

$$\int_{\mathbb{R}^3} f(x,\xi,t) \begin{pmatrix} 1 \\ \xi \\ \frac{|\xi|^2}{2} \end{pmatrix} d\xi = \begin{pmatrix} \rho(x,t) \\ \rho(x,t)U(x,t) \\ E(x,t) \end{pmatrix}$$

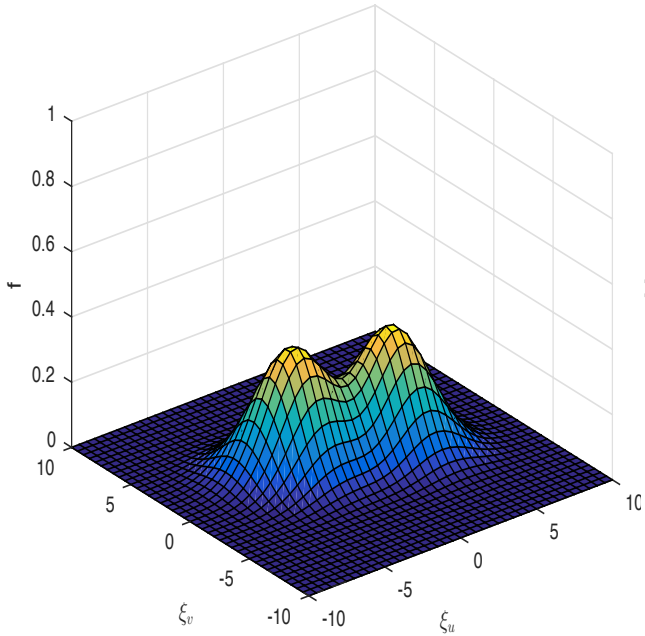
and the temperature is: $T(x,t) = \frac{2E(x,t)}{3\rho(x,t)} - \frac{|U(x,t)|^2}{3}$

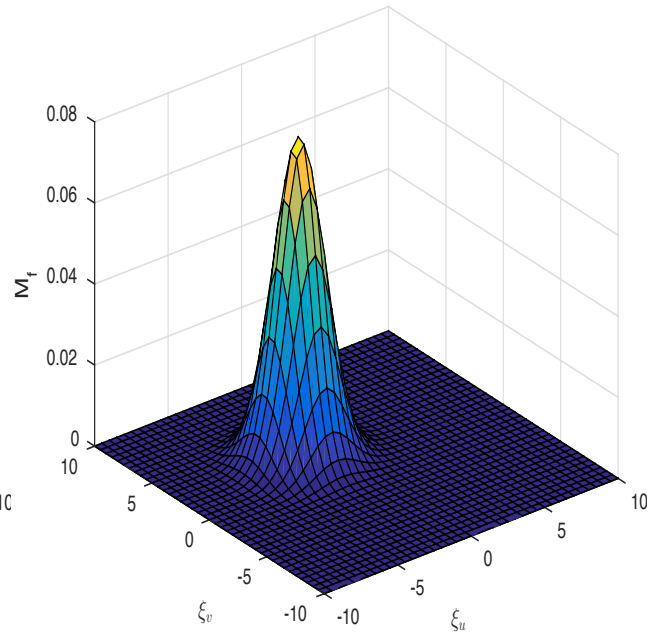
A.I., D. Lombardi PRE2011
F Bernard, A.I., S. Riffaud JCP2018

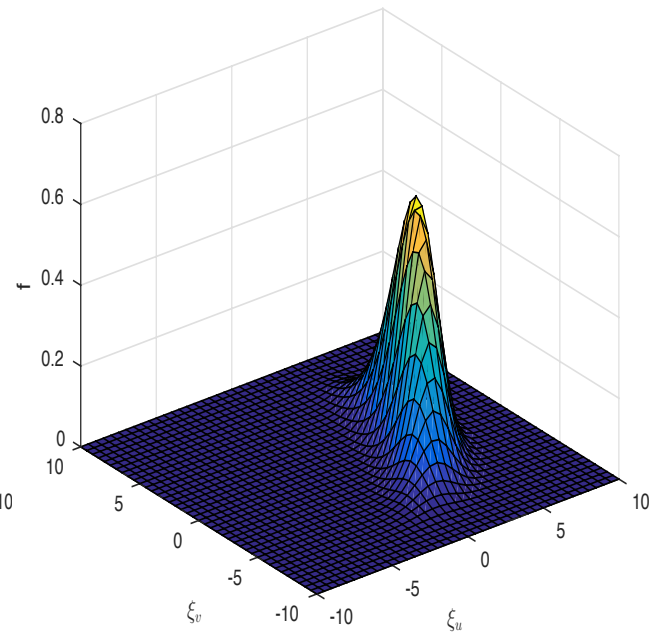
Sampling of the velocity density distributions

High-fidelity simulations provide snapshots of the distribution functions:

$$S^{\mathrm{hf}} = \left\{ f(\mathrm{x}_i, \xi, t_k) \right\}_{\substack{1 \le i \le N_{\mathbf{x}} \\ 1 \le k \le N_t}} \bigcup \left\{ M_f(\mathrm{x}_i, \xi, t_k) \right\}_{\substack{1 \le i \le N_{\mathbf{x}} \\ 1 \le k \le N_t}}$$



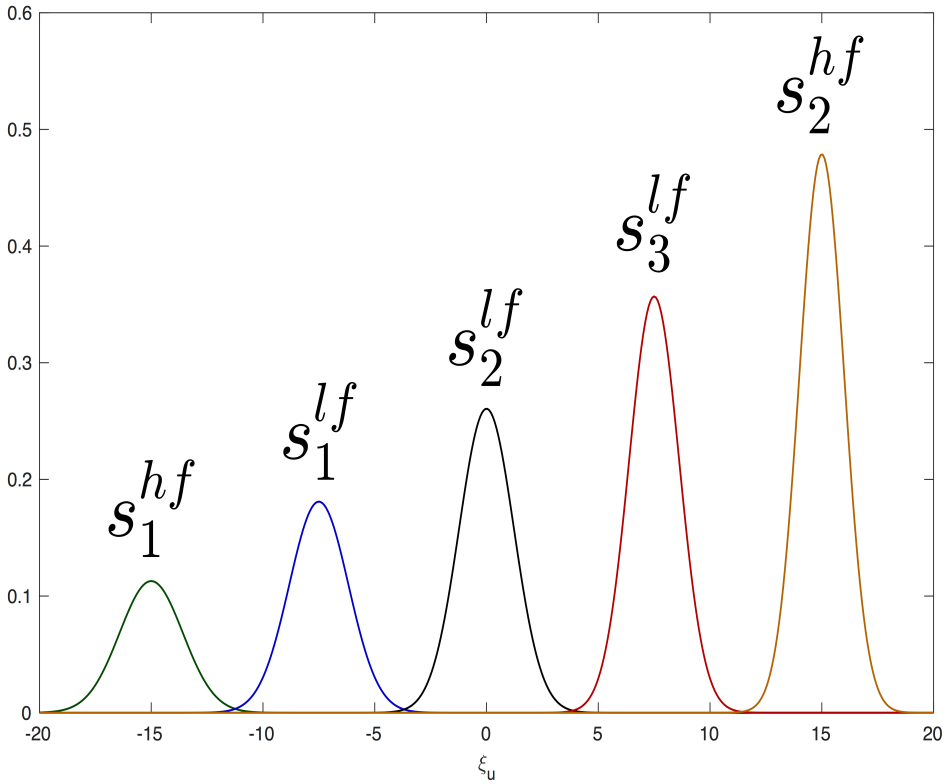




Data augmentation: Optimal Transportation

Optimal transportation provides additional low-fidelity snapshots by interpolating the snapshots of S^{hf} to complete the sampling:

$$S = S^{\text{hf}} \cup S^{\text{lf}}$$



Model reduction and Galerkin orthogonality

The distribution functions are represented by a small number of basis functions $\Phi_n(\xi)$ computed offline:

$$\widetilde{f}(x,\xi,t) = \sum_{n=1}^{N_{pod}} a_n^f(x,t)\Phi_n(\xi) \qquad \widetilde{M_f}(x,\xi,t) = \sum_{n=1}^{N_{pod}} a_n^M(x,t)\Phi_n(\xi)$$

Residual equation

$$\mathcal{R}(x,\xi,t) = \frac{\partial \widetilde{f}}{\partial t}(x,\xi,t) + \xi \cdot \nabla_x \widetilde{f}(x,\xi,t) - \frac{\widetilde{M_f}(x,\xi,t) - \widetilde{f}(x,\xi,t)}{\tau(x,t)}$$

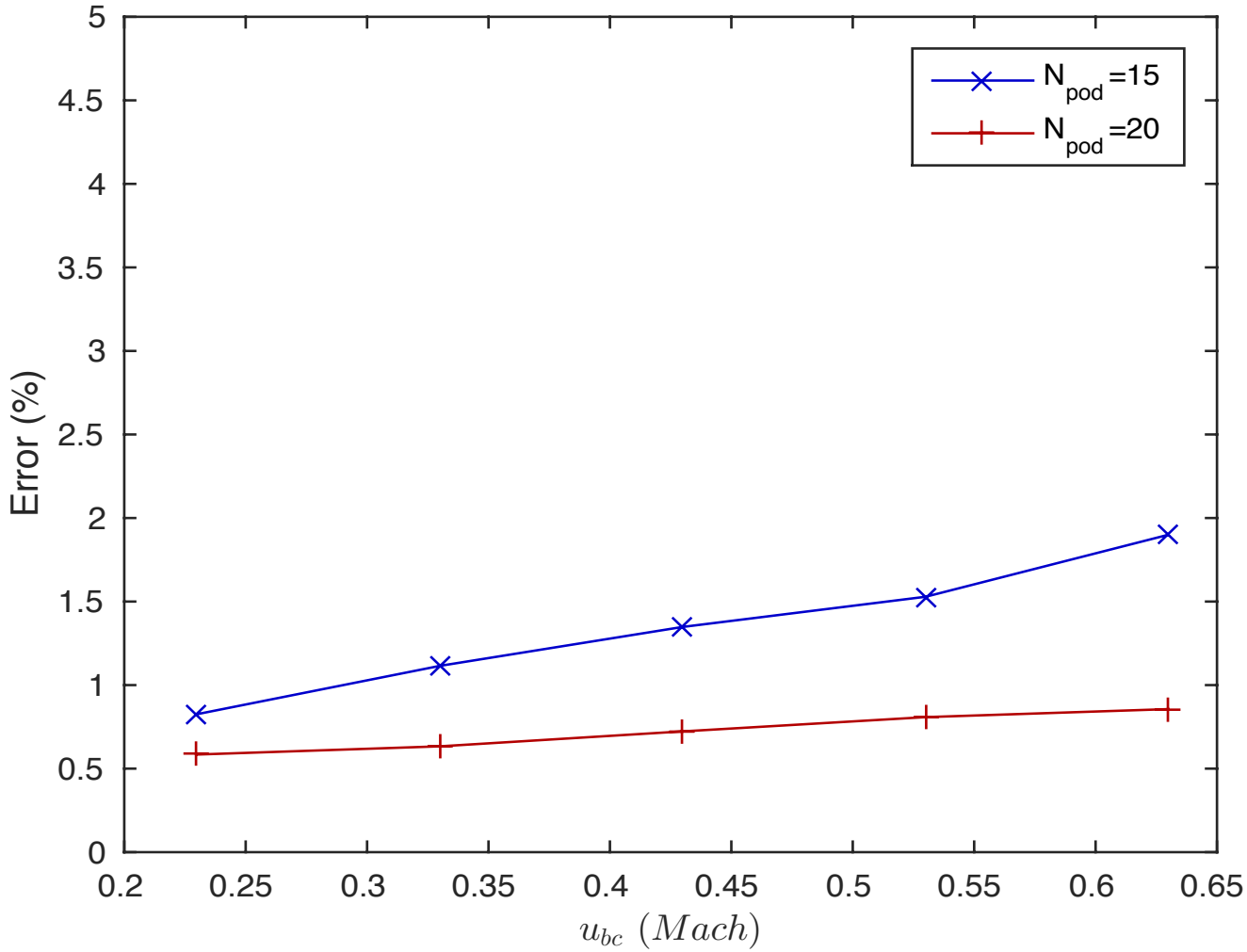
Orthogonality in the microscopic velocity space of $\mathcal{R}(x,\xi,t)$ to the subspace spanned by the columns of $\mathbf{\Phi}(\xi)$, $\Phi_n(\xi)$, $n = 1,\ldots,N_{pod}$:

$$< \mathcal{R}(x,\xi,t), \mathbf{\Phi}(\xi) >= 0$$

Rarefied flow past a flat plate

Prediction of a vortex flow as a function of the Mach number ($M_{bc} = 0.53$, $N_{pod} = 20$ and $Kn = 10^{-2}$).

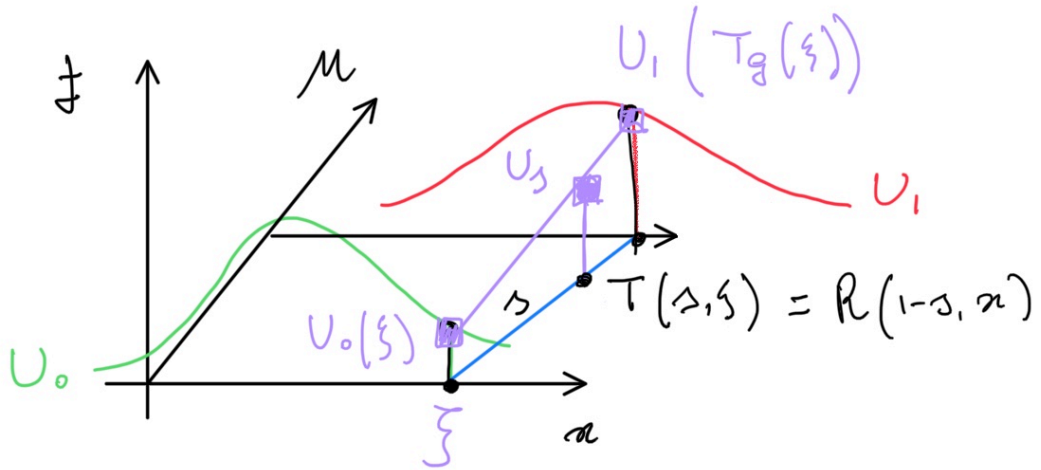
Rarefied flow past a flat plate: prediction error



Online computing time is divided by 50 for $N_{pod} = 15$ (and by 45 for $N_{pod} = 20$) on average.

Perspectives:
non-linear approximation spaces and non-intrusive approaches

Convex Displacement Interpolation



$$T(s,\cdot) = (1-s)\cdot + s\, T_g(\cdot) \quad ; \quad R_g = T_g^{-1}$$

$$R(s,\cdot) = (1-s)\cdot + s\, R_g(\cdot)$$

$$\boxed{U_t} = s\, U_1\left(T(1-s,x)\right) + (1-s)\, U_0\left(w(s,x)\right)$$

Symmetry
Interpolation

Gaussian model of coherent structures

- Given the field $U : \mathbb{R}^n \to \mathbb{R}^d$ and the scalar testing function $\mathcal{T}(\cdot; U) : \mathbb{R}^n \to \mathbb{R}$, the set

$$\mathcal{C}_{\mathcal{T}}(U) := \{x \in \mathbb{R}^n \, : \, \mathcal{T}(x; U) > 0\}$$

  identifies coherent structures associated with the criterion $\mathcal{T}$

Gaussian model of coherent structures

- Given the field $U : \mathbb{R}^n \to \mathbb{R}^d$ and the scalar testing function $\mathcal{T}(\cdot; U) : \mathbb{R}^n \to \mathbb{R}$, the set

$$\mathcal{C}_{\mathcal{T}}(U) := \{x \in \mathbb{R}^n \ : \ \mathcal{T}(x; U) > 0\}$$

  identifies coherent structures associated with the criterion $\mathcal{T}$
- For example, if U is a velocity field and $\mathcal{T}(x; U) = \|\nabla \times U(x)\|_2 - \tau$ with $\tau > 0$, $\mathcal{C}_{\mathcal{T}}(U)$ identifies the region where enstrophy exceeds a threshold τ

Gaussian model of coherent structures

- Given the field $U : \mathbb{R}^n \to \mathbb{R}^d$ and the scalar testing function $\mathcal{T}(\cdot; U) : \mathbb{R}^n \to \mathbb{R}$, the set

$$\mathcal{C}_{\mathcal{T}}(U) := \{x \in \mathbb{R}^n \ : \ \mathcal{T}(x; U) > 0\}$$

  identifies coherent structures associated with the criterion $\mathcal{T}$
- For example, if U is a velocity field and $\mathcal{T}(x; U) = \|\nabla \times U(x)\|_2 - \tau$ with $\tau > 0$, $\mathcal{C}_{\mathcal{T}}(U)$ identifies the region where enstrophy exceeds a threshold τ
- Objective: fit a Gaussian probability density function $\phi(x; \mu, \Sigma)$ to $\mathcal{C}_{\mathcal{T}}(U)$

$$\phi(x; \mu, \Sigma) = \frac{1}{(2\pi)^{n/2} |\Sigma|^{1/2}} \, e^{-\frac{1}{2}(x-\mu)^\top \Sigma^{-1}(x-\mu)}.$$

Gaussian model of coherent structures

- Given the field $U : \mathbb{R}^n \to \mathbb{R}^d$ and the scalar testing function $\mathcal{T}(\cdot; U) : \mathbb{R}^n \to \mathbb{R}$, the set
$$\mathcal{C}_{\mathcal{T}}(U) := \{x \in \mathbb{R}^n \ : \ \mathcal{T}(x; U) > 0\}$$
identifies coherent structures associated with the criterion $\mathcal{T}$
- For example, if U is a velocity field and $\mathcal{T}(x; U) = \|\nabla \times U(x)\|_2 - \tau$ with $\tau > 0$, $\mathcal{C}_{\mathcal{T}}(U)$ identifies the region where enstrophy exceeds a threshold τ
- Objective: fit a Gaussian probability density function $\phi(x;\, \mu, \Sigma)$ to $\mathcal{C}_{\mathcal{T}}(U)$
$$\phi(x;\, \mu, \Sigma) = \frac{1}{(2\pi)^{n/2}\, |\Sigma|^{1/2}}\ e^{-\frac{1}{2}(x-\mu)^\top \Sigma^{-1}(x-\mu)}.$$
- Define a finite-dimensional discretization of the domain of interest $P_{\mathrm{hf}} = \{x_i\}_{i=1}^{N_{\mathrm{hf}}}$ and we define
$$P_{\mathrm{hf}}^{+} := \{x \in P_{\mathrm{hf}} \ : \ \mathcal{T}(x; U) > 0\} = \{y_j\}_{j=1}^{N_{\mathrm{hf}}^{+}}$$

A.I., T. Taddei 2021, Mapping of coherent structures in parameterized flows by learning optimal transportation with Gaussian models, arXiv

Gaussian model of coherent structures

- Assume that $\{y_j\}_j$ are IID realizations of a multivariate Gaussian distribution and estimate mean and variance by MLE:

$$g(x;U) := \phi\left(x;\mu_{\mathrm{mle}}[U],\Sigma_{\mathrm{mle}}[U]\right)$$

$$\begin{cases} \mu_{\mathrm{mle}}[U] = \dfrac{1}{N_{\mathrm{hf}}^{+}} \displaystyle\sum_{j=1}^{N_{\mathrm{hf}}^{+}} y_j, \\ \Sigma_{\mathrm{mle}}[U] = \dfrac{1}{N_{\mathrm{hf}}^{+}} \displaystyle\sum_{j=1}^{N_{\mathrm{hf}}^{+}} \left(y_j - \mu_{\mathrm{mle}}[U]\right)\left(y_j - \mu_{\mathrm{mle}}[U]\right)^T \end{cases}$$

Gaussian model of coherent structures

- Assume that $\{y_j\}_j$ are IID realizations of a multivariate Gaussian distribution and estimate mean and variance by MLE:

$$g(x; U) := \phi\left(x; \mu_{\mathrm{mle}}[U], \Sigma_{\mathrm{mle}}[U]\right)$$

$$\begin{cases} \mu_{\mathrm{mle}}[U] = \dfrac{1}{N_{\mathrm{hf}}^{+}} \displaystyle\sum_{j=1}^{N_{\mathrm{hf}}^{+}} y_j, \\ \Sigma_{\mathrm{mle}}[U] = \dfrac{1}{N_{\mathrm{hf}}^{+}} \displaystyle\sum_{j=1}^{N_{\mathrm{hf}}^{+}} \left(y_j - \mu_{\mathrm{mle}}[U]\right)\left(y_j - \mu_{\mathrm{mle}}[U]\right)^T \end{cases}$$

- Given the Gaussian densities $\pi = \phi(\cdot;\, \mu_0, \Sigma_0)$ and $\nu = \phi(\cdot;\, \mu_1, \Sigma_1)$, the displacement interpolant $\widehat{\phi}_s$ is Gaussian with mean and covariance given by

$$\mu_s = (1-s)\,\mu_0 + s\,\mu_1, \quad \Sigma_s = \Sigma_0^{-1/2}\left((1-s)\,\Sigma_0 + s\left(\Sigma_0^{1/2}\Sigma_1\Sigma_0^{1/2}\right)^{1/2}\right)^2\Sigma_0^{-1/2}$$

for all $s \in [0, 1]$

Gaussian model of coherent structures

- Assume that $\{y_j\}_j$ are IID realizations of a multivariate Gaussian distribution and estimate mean and variance by MLE:

$$g(x;U) := \phi\left(x;\mu_{\mathrm{mle}}[U],\Sigma_{\mathrm{mle}}[U]\right)$$

$$\begin{cases} \mu_{\mathrm{mle}}[U] = \dfrac{1}{N_{\mathrm{hf}}^{+}} \displaystyle\sum_{j=1}^{N_{\mathrm{hf}}^{+}} y_j, \\ \Sigma_{\mathrm{mle}}[U] = \dfrac{1}{N_{\mathrm{hf}}^{+}} \displaystyle\sum_{j=1}^{N_{\mathrm{hf}}^{+}} \left(y_j - \mu_{\mathrm{mle}}[U]\right)\left(y_j - \mu_{\mathrm{mle}}[U]\right)^T \end{cases}$$

- Given the Gaussian densities $\pi = \phi(\cdot;\,\mu_0,\Sigma_0)$ and $\nu = \phi(\cdot;\,\mu_1,\Sigma_1)$, the displacement interpolant $\widehat{\phi}_s$ is Gaussian with mean and covariance given by

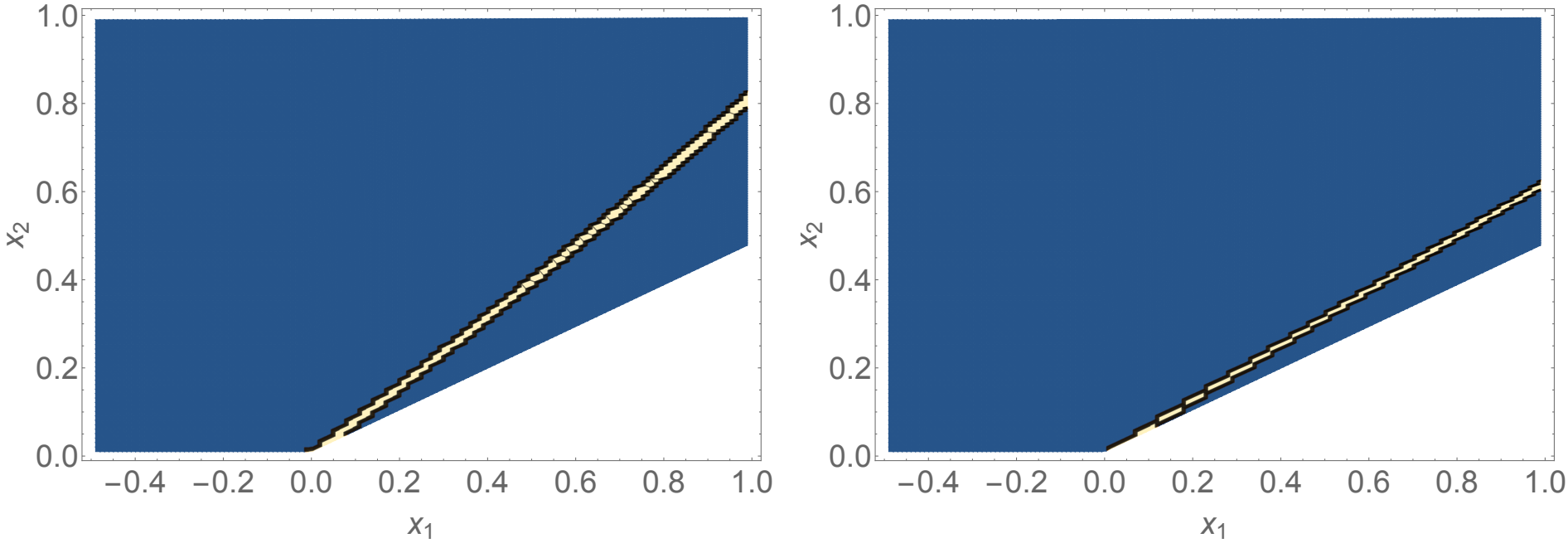
$$\mu_s = (1-s)\,\mu_0 + s\,\mu_1, \quad \Sigma_s = \Sigma_0^{-1/2}\left((1-s)\,\Sigma_0 + s\left(\Sigma_0^{1/2}\Sigma_1\Sigma_0^{1/2}\right)^{1/2}\right)^2\Sigma_0^{-1/2}$$

  for all $s \in [0,1]$

- The forward mapping T is also available in closed form:

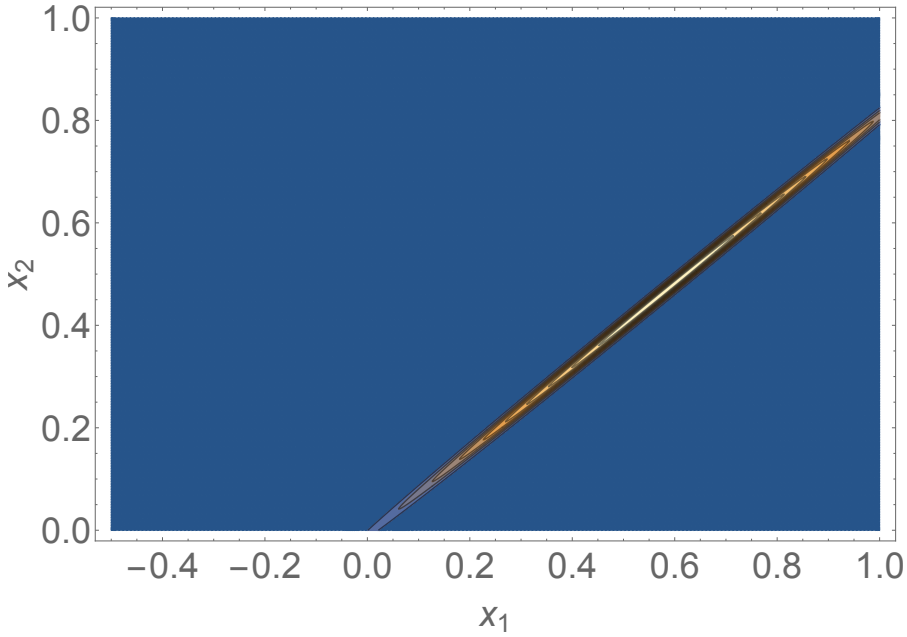
$$T(s,\xi) = (1-s)\,\xi + s\left(\mu_1 + \Sigma_0^{-1/2}\left(\Sigma_0^{1/2}\Sigma_1\Sigma_0^{1/2}\right)^{1/2}\Sigma_0^{-1/2}\left(\xi - \mu_0\right)\right)$$

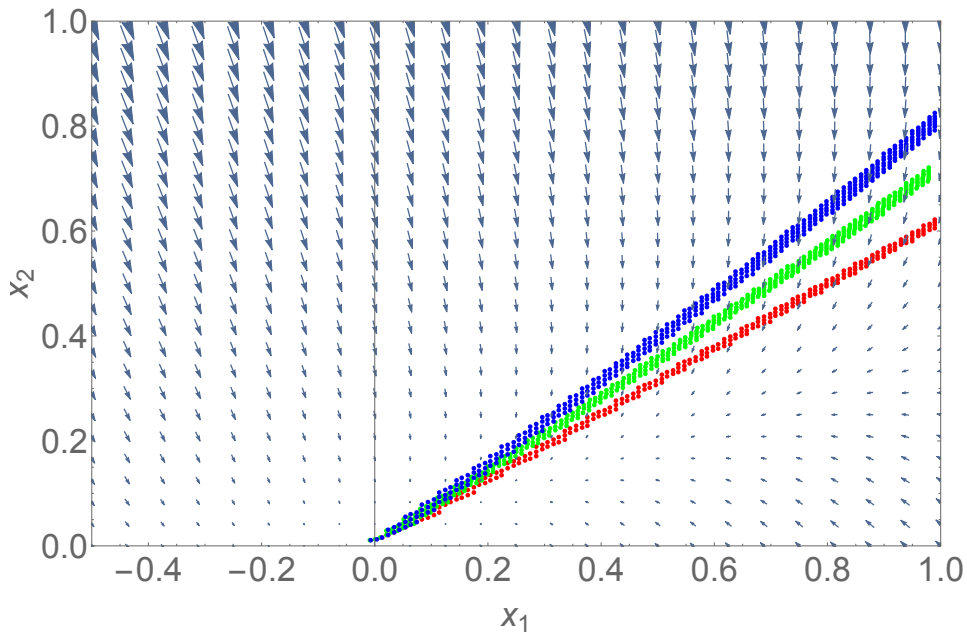
Supersonic wedge



Shocks in the mapped plane with wedge angle $(\delta_0 + \delta_1)/2$. Left: $M_0 = 5$, $\delta_0 = 28.275$ and shock angle on the physical plane of 40 degrees. Right: $M_1 = 8$, $\delta_1 = 22.80$ and a shock wave with angle of 30 degrees.

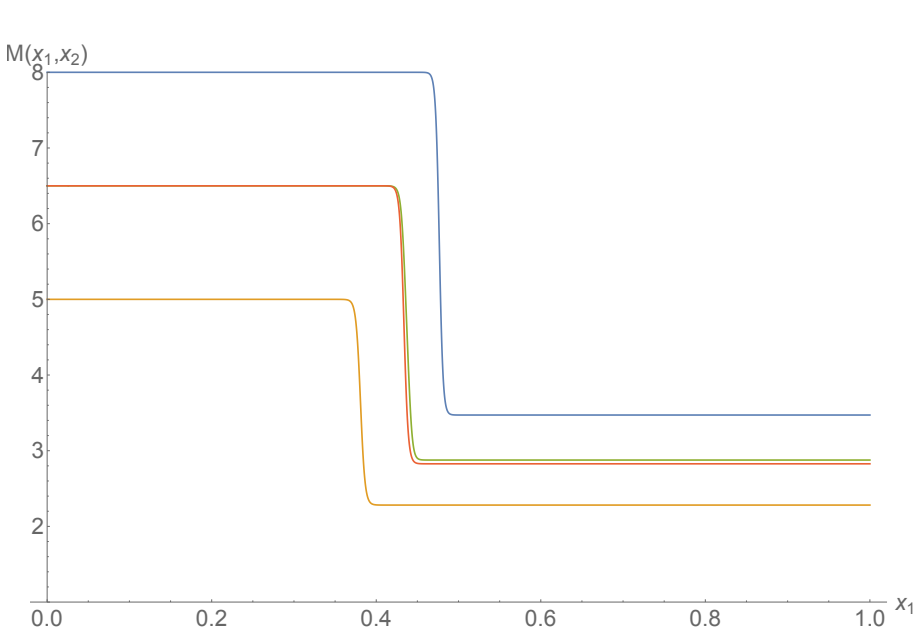
Supersonic wedge

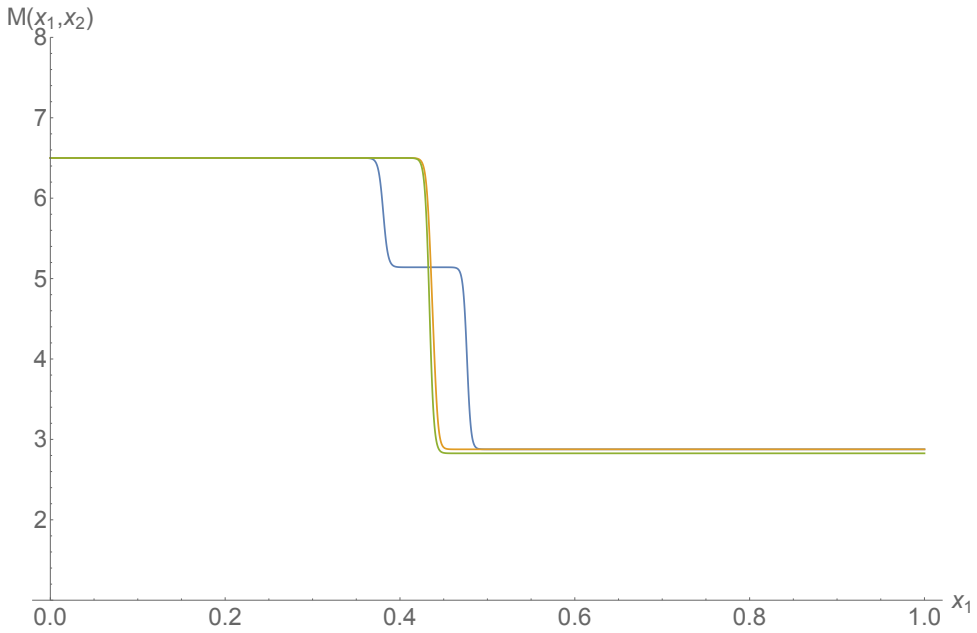




Left: Gaussian distribution corresponding to the 40 deg shock (second wedge) represented in the mapped plane with wedge angle $(\delta_0 + \delta_1)/2$. Right: optimal transportation map vector plot and points $\mathcal{P}^h_{\mathcal{T}}$ for the first wedge (red), the second (blue) and the points corresponding to the displacement interpolation with $\alpha = 1/2$ (green).

Supersonic wedge





Left: $\alpha = 1/2$. Right: $\alpha = 1/2$. Convex interpolation of exact solutions for M_0, δ_0 and M_1, δ_1 (blue). Exact solution (green) and convex displacement interpolant (orange).

Boundaries ?

Boundary-aware transportation of Gaussian models

- Given $M \in \mathbb{N}$, we introduce the approximation map $\mathcal{N} : \Omega \times \mathbb{R}^M \to \mathbb{R}^2$ and the set $\mathcal{A}_{\mathrm{bj}} \subset \mathbb{R}^M$ such that $\mathcal{N}(\cdot, \mathrm{a})$ is a bijection in Ω for all $\mathrm{a} \in \mathcal{A}_{\mathrm{bj}}$.

Boundary-aware transportation of Gaussian models

- Given $M \in \mathbb{N}$, we introduce the approximation map $\mathcal{N} : \Omega \times \mathbb{R}^M \to \mathbb{R}^2$ and the set $\mathcal{A}_{\mathrm{bj}} \subset \mathbb{R}^M$ such that $\mathcal{N}(\cdot, \mathrm{a})$ is a bijection in Ω for all $\mathrm{a} \in \mathcal{A}_{\mathrm{bj}}$.
- We denote by $P_{\mathrm{hf}}^{+,0} = \{y_j^0\}_{j=1}^{N_{\mathrm{hf},0}^+}$ and $P_{\mathrm{hf}}^{+,1} = \{y_j^1\}_{j=1}^{N_{\mathrm{hf},0}^+}$ the selected points for U_0 and U_1, and we denote by T_g and R_g the optimal maps obtained using the GMM.

Boundary-aware transportation of Gaussian models

- Given $M \in \mathbb{N}$, we introduce the approximation map $\mathcal{N} : \Omega \times \mathbb{R}^M \to \mathbb{R}^2$ and the set $\mathcal{A}_{\mathrm{bj}} \subset \mathbb{R}^M$ such that $\mathcal{N}(\cdot, \mathsf{a})$ is a bijection in Ω for all $\mathsf{a} \in \mathcal{A}_{\mathrm{bj}}$.
- We denote by $P_{\mathrm{hf}}^{+,0} = \{y_j^0\}_{j=1}^{N_{\mathrm{hf},0}^+}$ and $P_{\mathrm{hf}}^{+,1} = \{y_j^1\}_{j=1}^{N_{\mathrm{hf},0}^+}$ the selected points for U_0 and U_1, and we denote by T_g and R_g the optimal maps obtained using the GMM.
- We define $\widehat{\mathsf{a}}_{0,1} \in \mathbb{R}^M$ to minimize

$$\sum_{j=1}^{N_{\mathrm{hf},0}^+} \| T_g(y_j^0) - \mathcal{N}(y_j^0, \mathsf{a}) \|_2^2 + \mathcal{P}(\mathsf{a}), \quad \text{subject to } \mathcal{C}(\mathsf{a}) \leq 0,$$

where $\mathcal{P}$ is a suitable regularization that penalizes the H^2 seminorm of the mapping and $\mathcal{C}$ is a bijectivity constraint that, combined with $\mathcal{P}$, enforces that $\widehat{\mathsf{a}}_{0,1}$ belongs to $\mathcal{A}_{\mathrm{bj}}$. Similarly, we define $\widehat{\mathsf{a}}_{1,0} \in \mathbb{R}^M$ to minimize

$$\sum_{j=1}^{N_{\mathrm{hf},1}^+} \| R_g(y_j^1) - \mathcal{N}(y_j^1, \mathsf{a}) \|_2^2 + \mathcal{P}(\mathsf{a}), \quad \text{subject to } \mathcal{C}(\mathsf{a}) \leq 0.$$

Transonic airfoil

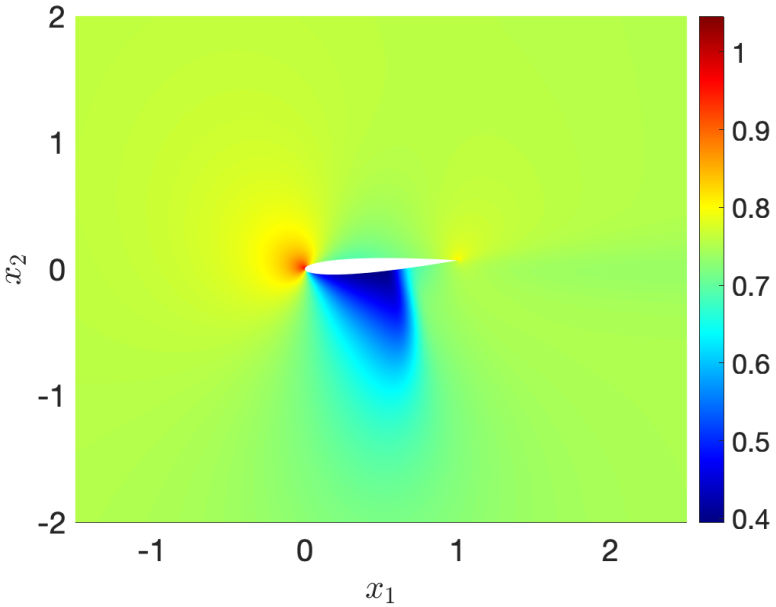
We introduce the boundary-aware (BA) convex displacement interpolation as

$$\widehat{U}(s,x) \;=\; (1-s)U_0 \circ \widetilde{W}_g(s,x) \;+\; sU_1 \circ \widetilde{T}_g(1-s,x), \quad s \in [0,1],\; x \in \Omega,$$

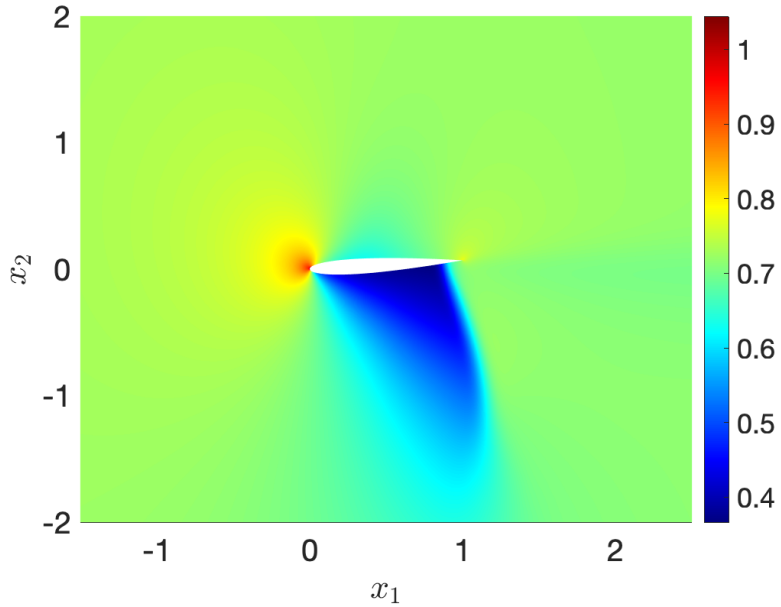
$$\text{where } \widetilde{T}_g(s,x) = \mathcal{N}(x,\, s \cdot \widehat{\mathrm{a}}_{0,1}) \text{ and } \widetilde{W}_g(s,x) = \mathcal{N}(x,\, s \cdot \widehat{\mathrm{a}}_{1,0}).$$

Transonic airfoil

NACA 0012 airfoil at angle of attack $\alpha = -4^o$; free-stream Mach number $M \in [0.77, 0.83]$; we study the interpolation between $M_0 = 0.77$ and $M_1 = 0.83$.



(a) $M = 0.77$



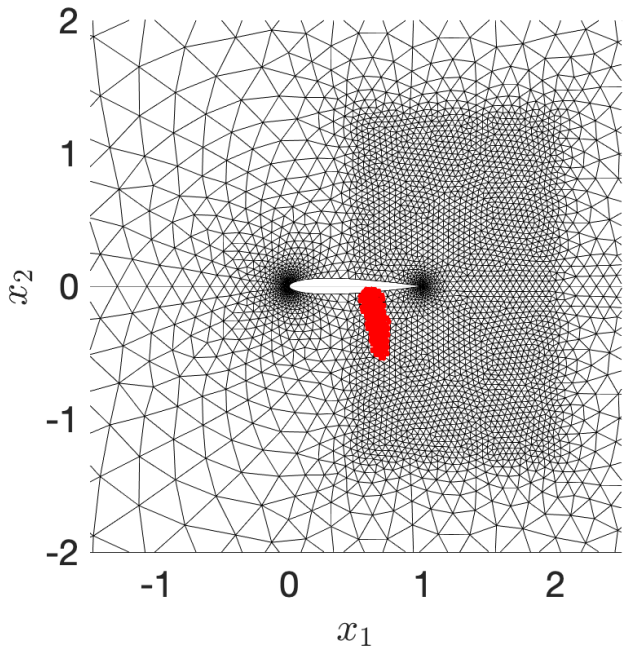
(b) $M = 0.83$

Transonic airfoil

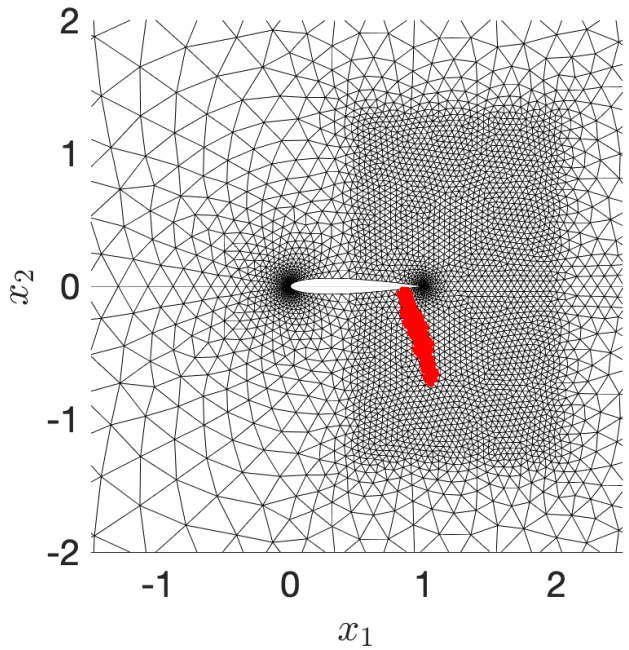
Modified Ducros shock indicator:

$$d_k = \max_{x \in \mathtt{D}_k} \left|\phi(x;U)\right|, \quad \phi(x;U) := \frac{(-\nabla \cdot u)^+}{\sqrt{(\nabla \cdot u)^2 + \|\nabla \times u\|_2^2 + a^2}} \frac{\|\nabla p\|_2}{p+\epsilon} \|u\|_2$$

where $\mathtt{D}_k$ denotes the k-th element of the DG mesh, $k = 1, \ldots, N_\mathrm{e}$, and $\epsilon = 10^{-4}$; then, we define P_hf^+ as the set associated with the largest 0.5% values of the indicator $\{d_k\}_{k=1}^{N_\mathrm{e}}$.



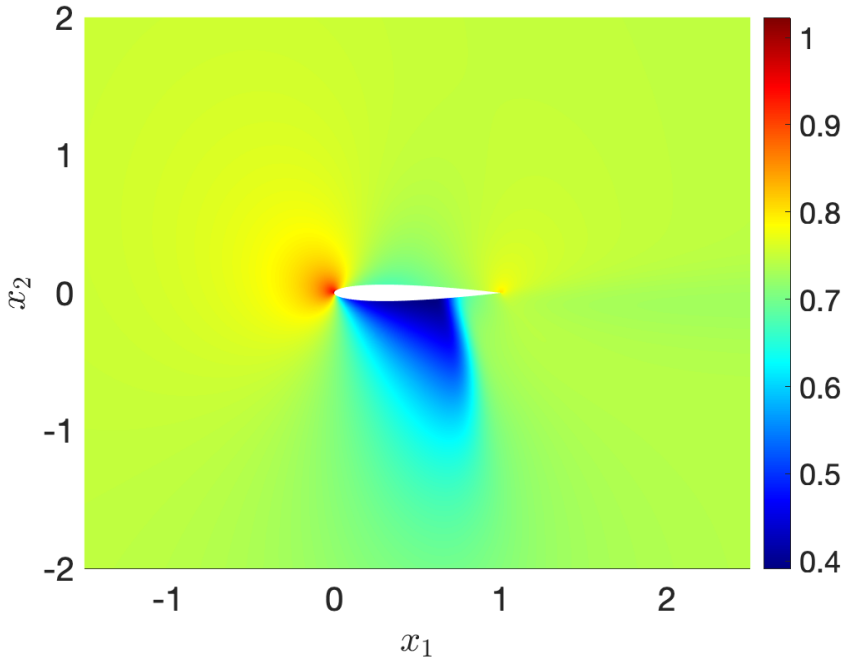
(a) $M = 0.77$



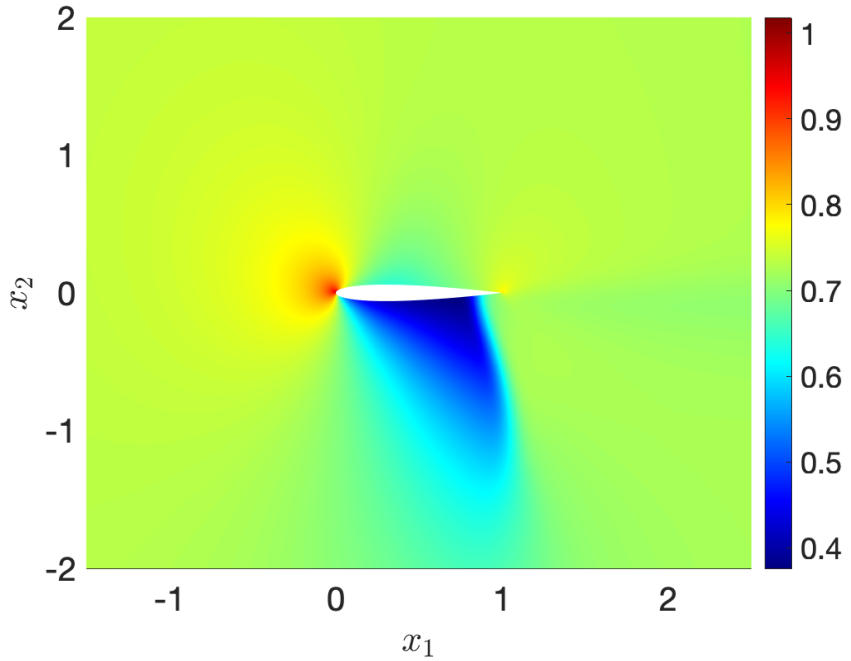
(b) $M = 0.83$

Transonic airfoil

The proposed interpolation preserves the structures at leading and trailing edges and is able to smoothly deform the shock attached to the airfoil.

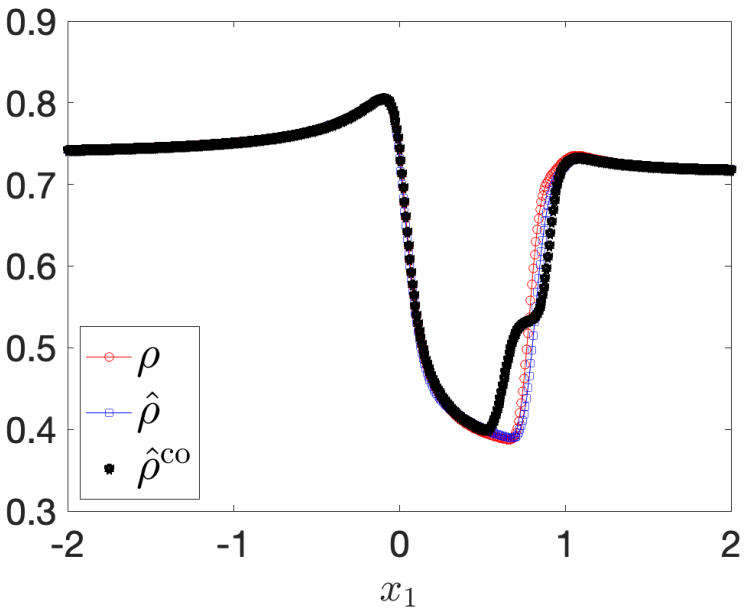


(a) $s = 0.25$

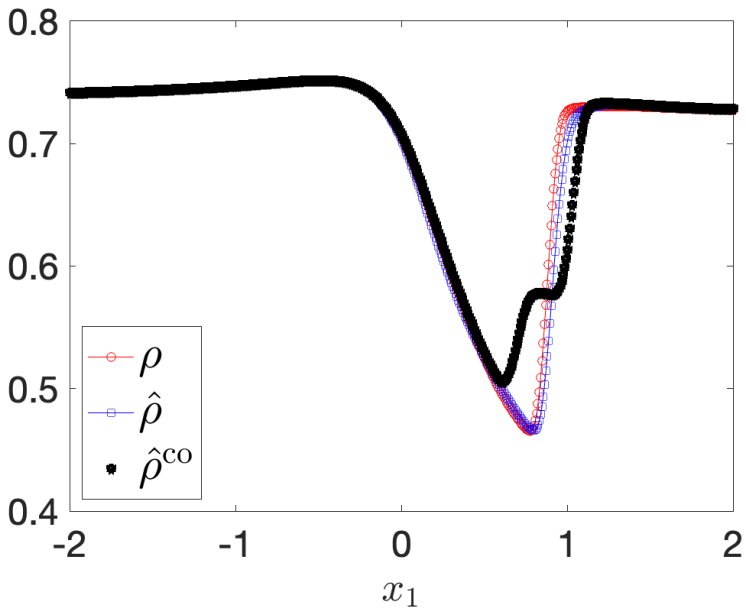


(b) $s = 0.75$

Transonic airfoil



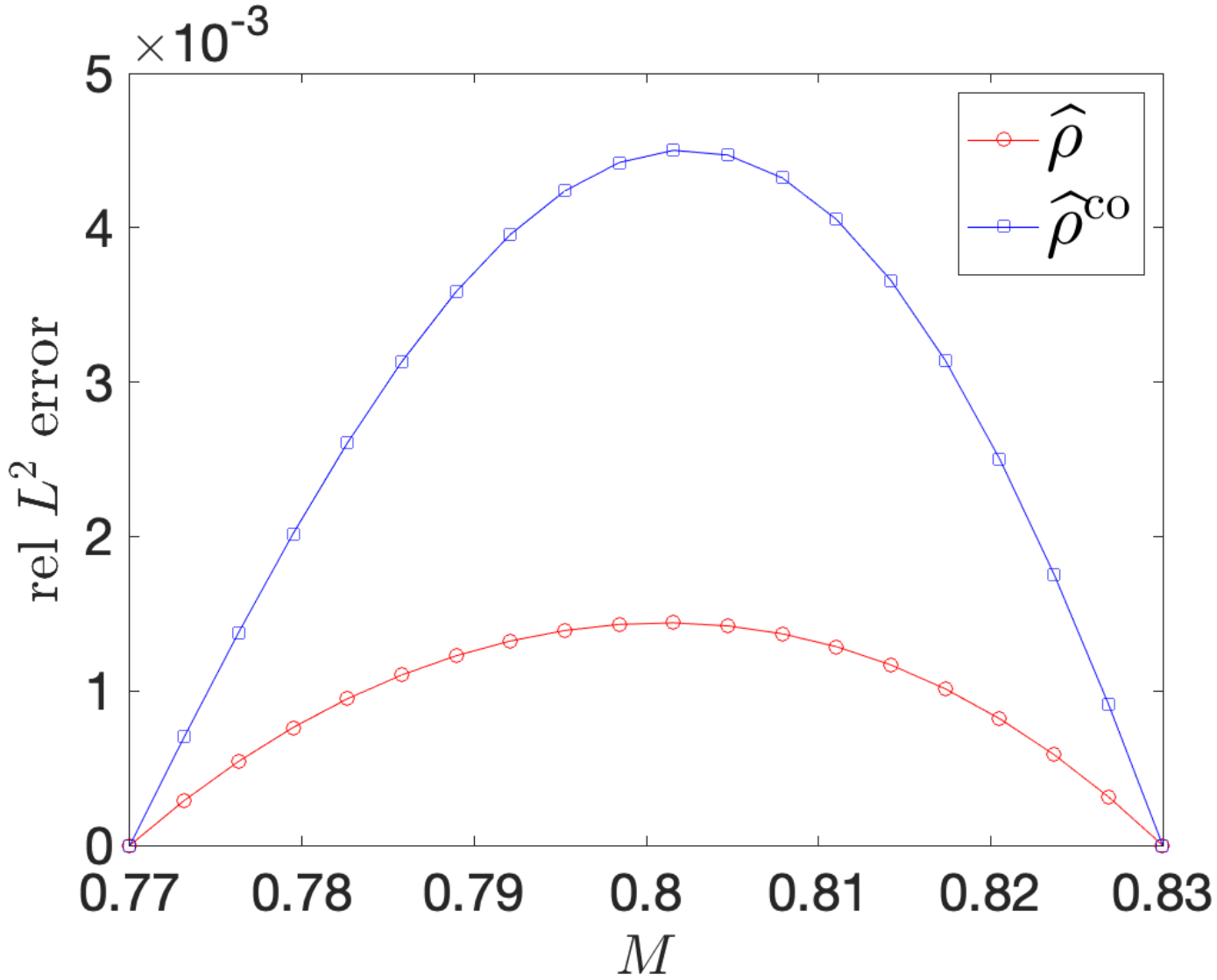
(a) $x_2 = -0.1$



(b) $x_2 = -0.5$

boundary-aware transportation of Gaussian models (angle of attack 4^o). (a)-(b) horizontal slices of truth and predicted density profiles for $M = 0.8$.

Transonic airfoil



Conclusions

- Old & New. Explicable models: computational science & data

Conclusions

- Old & New. Explicable models: computational science & data
- Learning: approximation space, residual collocation, hybrid discretization, data augmentation

Conclusions

- Old & New. Explicable models: computational science & data
- Learning: approximation space, residual collocation, hybrid discretization, data augmentation
- Non-linear interpolation spaces & non-intrusive approaches